Chapter 6. Terrestrial Carbon Modeling: Baseline and Projections in Upland Ecosystems

By Hélène Genet,[1] Yujie He,[2] A. David McGuire,[3] Qianlai Zhuang,[2] Yujin Zhang,[1], Frances E. Biles,[4] David V. D'Amore,[4] Xiaoping Zhou,[5] and Kristopher D. Johnson[6]

6.1. Highlights

- Ecosystem carbon balance of the Alaska assessment domain (as outlined in chapter 1) was examined using a process-based model framework for two time periods: a historical period (1950–2009), for which historical climate and disturbance observations were used, and a projection period (2010–2099), for which projected climate and disturbance data were used.
- During the historical period, upland ecosystems in Alaska were a net carbon sink of an average of 5.01 teragrams of carbon per year (TgC/yr). All Landscape Conservation Cooperative (LCC) regions in Alaska were net carbon sinks, except for the Northwest Boreal LCC North. This carbon sink was mostly due to an increase in vegetation productivity associated with recent warming.
- For the Northwest Boreal LCC North, the carbon source averaged –5.12 TgC/yr and was associated with large carbon losses from wildfire, specifically during large fire years in 1957, 1969, 1977, 1990–1991, 2004, and 2005.
- Carbon loss from forest harvest exports in the North Pacific LCC represented 1.6 percent of the statewide gross carbon losses between 1950 and 2009.
- During the projection period (2010–2099), all LCC regions of Alaska were projected to be carbon sinks, storing between 14.72 and 30.15 TgC/yr statewide.
- Methane consumption in upland ecosystems was projected to be low relative to gross primary productivity (GPP), representing on average 0.0011 percent of the projected GPP by 2099.
- Disturbances, mainly wildfires, would be a strong determinant of the future spatial and temporal variability of carbon dynamics, particularly in the Northwest Boreal LCC North.

6.2. Introduction

Arctic and boreal permafrost soils hold about 1,700 petagrams of organic carbon (Zimov and others, 2006; Schuur and others, 2008; Tarnocai and others, 2009), more than twice the carbon in atmospheric carbon dioxide (CO_2). Thus, changes in the carbon balance of permafrost ecosystems in response to climate warming could profoundly alter the composition of the atmosphere to affect the climate system (Schaefer and others, 2011; Schuur and others, 2013). As permafrost warms, organic matter that has been frozen for hundreds to thousands of years is exposed to microbial decomposition, mineralization, and release to the atmosphere as CO_2 and methane (CH_4) greenhouse gases that may offset carbon gain from potential increases in vegetation productivity in response to climate warming.

[1]University of Alaska-Fairbanks, Fairbanks, Alaska.

[2]Purdue University, West Lafayette, Ind.

[3]U.S. Geological Survey, Fairbanks, Alaska.

[4]U.S. Department of Agriculture Forest Service, Juneau, Alaska.

[5]U.S. Department of Agriculture Forest Service, Portland, Oreg.

[6]U.S. Department of Agriculture Forest Service, Newtown Square, Pa.

Boreal and arctic regions are thought to have been a strong carbon sink during the 20th century (McGuire and others, 2009; Pan and others, 2011). More recent analyses that included consideration of the last decade of intensive fire activity throughout the boreal zone and CH_4 emissions in the region indicate that the carbon sink is weakening and that the region is acting as a net source of greenhouse gases when the global warming potential of CH_4 is considered (McGuire and others, 2010; Hayes and others, 2011). A recent analysis of historical carbon exchange in arctic tundra (1990–2006), using observations, regional and global applications of process-based models, and atmospheric inversion models, suggests that large uncertainties existed that could not be distinguished from neutral balance (McGuire and others, 2012). One of the sources of this uncertainty is related to the weak ability of process-based models to represent the temporal variability of carbon dynamics across the landscape (Fisher and others, 2014). In Alaska, the spatial and temporal variability of carbon dynamics depend primarily on drainage conditions and disturbance regimes (Schuur and others, 2009; Tarnocai and others, 2009; Grosse and others, 2011). Indeed, uplands and wetlands are dominated by different soil carbon processes; vegetation productivity; and nature, frequency, and severity of disturbance regimes.

In this report, we review the main drivers of carbon dynamics separately for uplands (this chapter) and wetlands (chapter 7). Uplands in Alaska are characterized by moderately to well drained ecosystems composed of forest and alpine ecosystems in the boreal and maritime regions and the tundra ecosystem in the arctic region. Because of good drainage conditions, soil biogeochemical dynamics in uplands are dominated by aerobic processes (Schuur and others, 2009). Carbon and nutrient turnover is faster and the vegetation is generally more productive in uplands than in wetlands. In past syntheses of regional carbon dynamics, the role of aerated soils as a sink for atmospheric CH_4 has been neglected. However, it has been documented that CH_4 consumption exceeds CH_4 production in moist tundra soils of Alaska (Whalen and Reeburgh, 1990). Therefore, for a comprehensive assessment of carbon dynamics in northern high latitudes, it is important to consider CH_4 uptake in uplands. Wildfire and forest harvest are two important disturbance regimes in uplands in Alaska. Whereas wildfire occurs mostly in boreal forest and to a lesser extent in arctic tundra (Mack and others, 2011; Turetsky and others, 2011), forest harvest is concentrated in southern coastal Alaska. Annual area burned has increased in Alaska (Kasischke and Turetsky 2006; Kasischke and others, 2010) and Canada (Gillett and others, 2004) during the second half of the 20th century. In Alaska, the decade beginning in 2000 experienced the highest burned area (76,700 square kilometers per year [km^2/yr]) during the modern record period (baseline at 39,970 km^2/yr from 1920 to 2009). In Canada, average burned area increased continuously from the 1940s (81,650 km^2/yr) through the 1990s (317,070 km^2/yr) before sharply decreasing in the 2000s (165,430 km^2/yr). Several studies indicate that this increase is predicted to be maintained at least during the first half of the 21st century (Balshi and others, 2009; Mann and others, 2012; chapter 2). In addition to an increase in carbon emissions from burning, greater fire frequency and severity have substantial implications for permafrost, as increased severity leads to greater consumption of the insulating organic layer, which may accelerate permafrost thaw and associated deep carbon decomposition (Dyrness and Norum, 1983; Yoshikawa and others, 2002; Burn and others, 2009). Finally, commercial harvesting of maritime upland forest (that is, western hemlock [*Tsuga heterophylla* (Raf.) Sarg.] and Sitka spruce [*Picea sitchensis* (Bong.) Carrière]) in southeast and south-central Alaska has been developing since the late 19th century (Rakestraw, 1981; chapter 5). Although harvesting reduces aboveground carbon stocks by exporting wood out of the ecosystem, it might promote vegetation productivity by increasing areas of secondary growth (Cole and others, 2010).

In this chapter, we assess historical and projected carbon dynamics of upland ecosystems in Alaska by using a modeling framework that combines process-based biogeochemical and biogeographic-disturbance models at a spatial resolution of 1 kilometer (km). We evaluated the long-term consequences of a projected warming and disturbance regime on the regional carbon balance in uplands in Alaska from 2009 to 2099 using six climate simulations from two general circulation models (GCMs) for three atmospheric CO_2 emissions scenarios.

6.3. Material and Methods

6.3.1. Model Framework

Changes in soil and vegetation carbon stocks and fluxes in response to climate change and disturbances were analyzed using a modeling framework that combines a wildfire disturbance model, the Alaska Frame-Based Ecosystem Code (ALFRESCO; Rupp and others, 2000, 2002, 2007; Johnstone and others, 2011; Mann and others, 2012; Gustine and others, 2014; Amy Breen, University of Alaska-Fairbanks, written commun., 2015), and two process-based ecosystem models that simulate (1) carbon and nitrogen pools and CO_2 dynamics using the Dynamic Organic Soil version of the Terrestrial Ecosystem Model (DOS-TEM; Raich and others, 1991; McGuire and others, 1992) and (2) CH_4 dynamics using the Methane Dynamics Module of the Terrestrial Ecosystem Model (MDM-TEM; Zhuang and others, 2004). These three models have been coupled in an asynchronous way, in which the time series of fire occurrence simulated by ALFRESCO is used to drive DOS-TEM, which simulates the effects of wildfire, warming, and forest harvest on carbon pools and aerobic carbon processes. Monthly net primary productivity (NPP) and leaf area index (LAI) simulated by DOS-TEM are used to drive MDM-TEM, which simulates anaerobic (methanogenesis) and aerobic (methane oxidation) carbon processes (fig. 6.1). Description of the ALFRESCO model is provided in chapter 2, section 2.3.2. As MDM-TEM

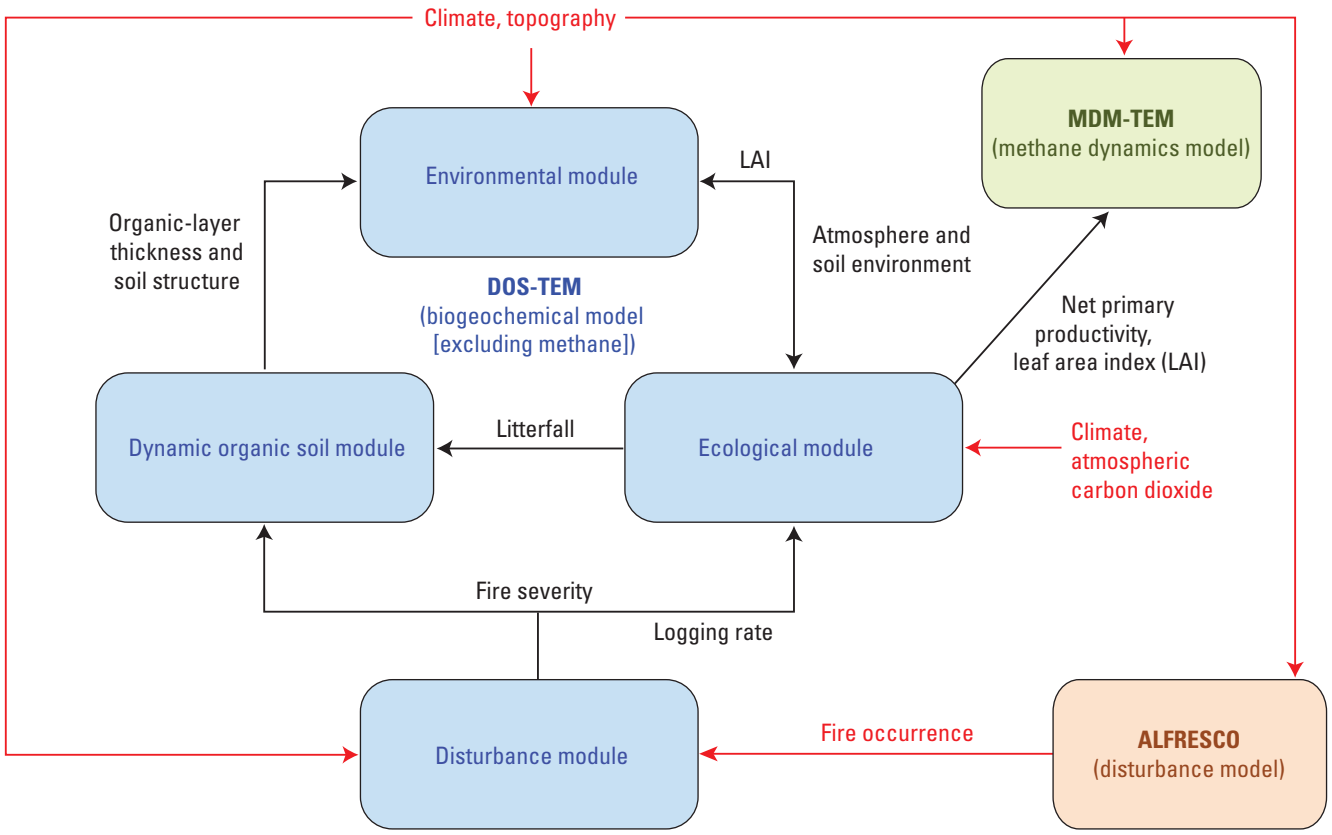

Figure 6.1. Modeling framework for this assessment. Red text and arrows represent input drivers. Black text and arrows represent flows of information within and among models. Blue boxes represent the four modules composing the Dynamic Organic Soil version of the Terrestrial Ecosystem Model (DOS-TEM). The orange box represents the disturbance model Alaska Frame-Based Ecosystem Code (ALFRESCO) and the green box represents the methane dynamics model Methane Dynamics Module of the Terrestrial Ecosystem Model (MDM-TEM).

simulations are of particular importance for simulating wetland carbon dynamics, the MDM-TEM model is described in chapter 7, section 7.3.1. Here we focus on descriptions of DOS-TEM for upland carbon modeling.

6.3.2. Dynamic Organic Soil Version of the Terrestrial Ecosystem Model (DOS-TEM) Description

DOS-TEM belongs to the Terrestrial Ecosystem Model (TEM) family of process-based ecosystem models that has been designed to simulate carbon and nitrogen pools in vegetation and soil, and carbon and nitrogen fluxes among vegetation, soil, and the atmosphere (Raich and others, 1991; McGuire and others, 1992). DOS-TEM is composed of four modules: an environmental module, an ecological module, a disturbance module, and a dynamic organic soil module.

The environmental module computes dynamics of biophysical processes in the soil and the atmosphere, driven by climate and soil texture input data, leaf area index from the ecological module, and soil structure from the dynamic organic soil module. Soil temperature and moisture conditions are calculated for multiple layers within various soil horizons, including moss, fibric and humic organic layers, and mineral horizons. A stable snow/soil thermal model integrated into the environmental module uses the Two-Directional Stefan Algorithm (TDSA; Woo and others, 2004). The TDSA can satisfactorily simulate the positions of the freeze-thaw front and active-layer thickness in a land surface model when proper surface forcing is provided (Yi and others, 2006). The environmental module provides information regarding the atmospheric and soil environment to the ecological module and the disturbance module.

The ecological module simulates carbon and nitrogen dynamics among the atmosphere, the vegetation, and the soil. Carbon and nitrogen dynamics are driven by climate input data, information on soil and atmospheric environment from the environmental module, information on soil structure provided by the dynamic organic soil module, and information on timing and severity of wildfire or forest harvest occurrences provided by the disturbance module.

The dynamic organic soil module calculates the thickness of the fibric and humic organic layers after soil carbon pools are altered by ecological processes (litterfall, decomposition, and burial) and fire disturbance. The estimation of organic

horizon thickness is computed from soil carbon content using relationships that link soil organic carbon content and soil organic thickness (Yi, McGuire, and others, 2009). These relationships have been developed for fibric, humic, and mineral horizons for every vegetation type, based on data from the soil carbon network database for Alaska (Johnson and others, 2011). Once the thickness of each organic soil horizon is estimated, the dynamic organic soil module calculates the number of layers in each organic horizon and the thickness of each layer to maintain stability and efficiency of soil temperature and moisture calculations along the soil column, as a function of the soil characteristics of each layer.

Finally, the disturbance module simulates how forest harvest and wildfire affect carbon and nitrogen pools of the vegetation and the soil. For wildfire, the module computes combustion emissions to the atmosphere, the fate of uncombusted carbon and nitrogen pools, and the flux of nitrogen from the atmosphere to the soil via biological nitrogen fixation in the years following a fire. The amount of soil carbon combusted during a wildfire is determined using input data on topography, drainage, and vegetation, as well as soil (moisture and temperature) and atmospheric (evapotranspiration) data from the environmental module (Genet and others, 2013).

Previous regional applications of DOS-TEM in northern high latitudes have investigated how biogeochemical dynamics of terrestrial ecosystems in these regions are affected at seasonal to century scales by processes like soil thermal activities (Zhuang and others, 2001, 2002, 2003), snow cover (Euskirchen and others, 2006, 2007), and fire (Balshi and others, 2007; Yuan and others, 2012). DOS-TEM has been developed primarily to represent the effects of disturbances, wildfire especially, on carbon stocks in vegetation and soil organic horizons and on the soil environment in permafrost regions (Yi, Manies, and others, 2009; Yi, McGuire, and others, 2009; Yi and others, 2010). Recent model developments have focused on the spatial and temporal heterogeneity of fire severity and carbon loss associated with the influence of drainage conditions, vegetation composition, topography, and weather conditions across the landscape (Genet and others, 2013). In this study, we developed an additional capability for DOS-TEM to consider the effects of forest harvest disturbance on carbon balance, which is described below.

6.3.3. Dynamic Organic Soil Version of the Terrestrial Ecosystem Model (DOS-TEM) Development—Modeling the Effect of Forest Harvest on Carbon Dynamics

For this assessment, we further developed the disturbance module of DOS-TEM to represent the effects of forest harvest on carbon and nitrogen dynamics. The harvesting of timber in southern coastal Alaska took place primarily between the mid-1950s and mid-1990s (fig. 6.2) when two pulp mills opened in Sitka and Ketchikan to process large volumes of low-grade timber, mainly from the Tongass National Forest where the U.S. Department of Agriculture (USDA) Forest Service began offering 50-year timber sale contracts (Colt and others, 2007). After 1990, the USDA Forest Service reduced the volume of timber offered for sale annually, and in 1997, the agency imposed harvest constraints that resulted in large increases in the cost of harvesting timber on national forest lands and a decrease of the annual volume harvested.

Forest harvest by clear-cutting was widespread in southeastern Alaska since the early 1950s (Alaback, 1982; Cole and others, 2010). We developed a harvesting module with an assumption that 95 percent of the aboveground vegetation biomass would be harvested (Deal and others, 2002). Among the residual biomass, 4 percent was considered dead and 1 percent alive to allow post-harvest recruitment. As a consequence, 99 percent of the belowground vegetation biomass (root biomass) was considered dead and transferred to the soil organic matter pool. Exported out of the ecosystem, the carbon in timber will mainly be stored in permanent constructions or furniture.

6.3.4. Model Parameterization and Validation

6.3.4.1. Dynamic Organic Soil Version of the Terrestrial Ecosystem Model (DOS-TEM)

Rate-limiting parameters of the model were calibrated for 11 main land-cover types in Alaska—4 types of tundra (graminoid, shrub, heath, and wet-sedge tundra), 3 types of boreal forest (black spruce [*Picea mariana* (Mill.) Britton, Sterns & Poggenb.], white spruce [*Picea glauca* (Moench) Voss], and deciduous forest), and 4 types of maritime communities (upland forest, wetland forest, fen, and alder shrubland). (See chapter 2, section 2.4.1 for further description of these land-cover types.) In boreal regions, similar vegetation composition can occur in very different drainage conditions leading to high variability in carbon and nitrogen turnover (Schuur and others, 2009; Wickland and others, 2010) and vulnerability to disturbance (Turetsky and others, 2011); therefore, the three types of boreal forest were calibrated separately for uplands and for wetlands. In this chapter, we focus on the calibration of upland ecosystems: graminoid tundra, shrub tundra, heath tundra, boreal upland black spruce forest, boreal upland white spruce forest, boreal upland deciduous forest, and maritime upland forest. (See chapter 7, section 7.3.2.3 for calibration of wetlands and lowland boreal forests.)

We calibrated the rate-limiting parameters of DOS-TEM using target values of carbon and nitrogen pools and fluxes representative of mature ecosystems. These parameters were "tuned" until the model reached target values of the main carbon and nitrogen pools and fluxes (Clein and others, 2002). The calibration of these parameters is an effective means of dealing with temporal scaling issues in ecosystem models (Rastetter and others, 1992). For boreal forest communities, an existing set of target values for vegetation and soil carbon and nitrogen pools and fluxes was assembled using

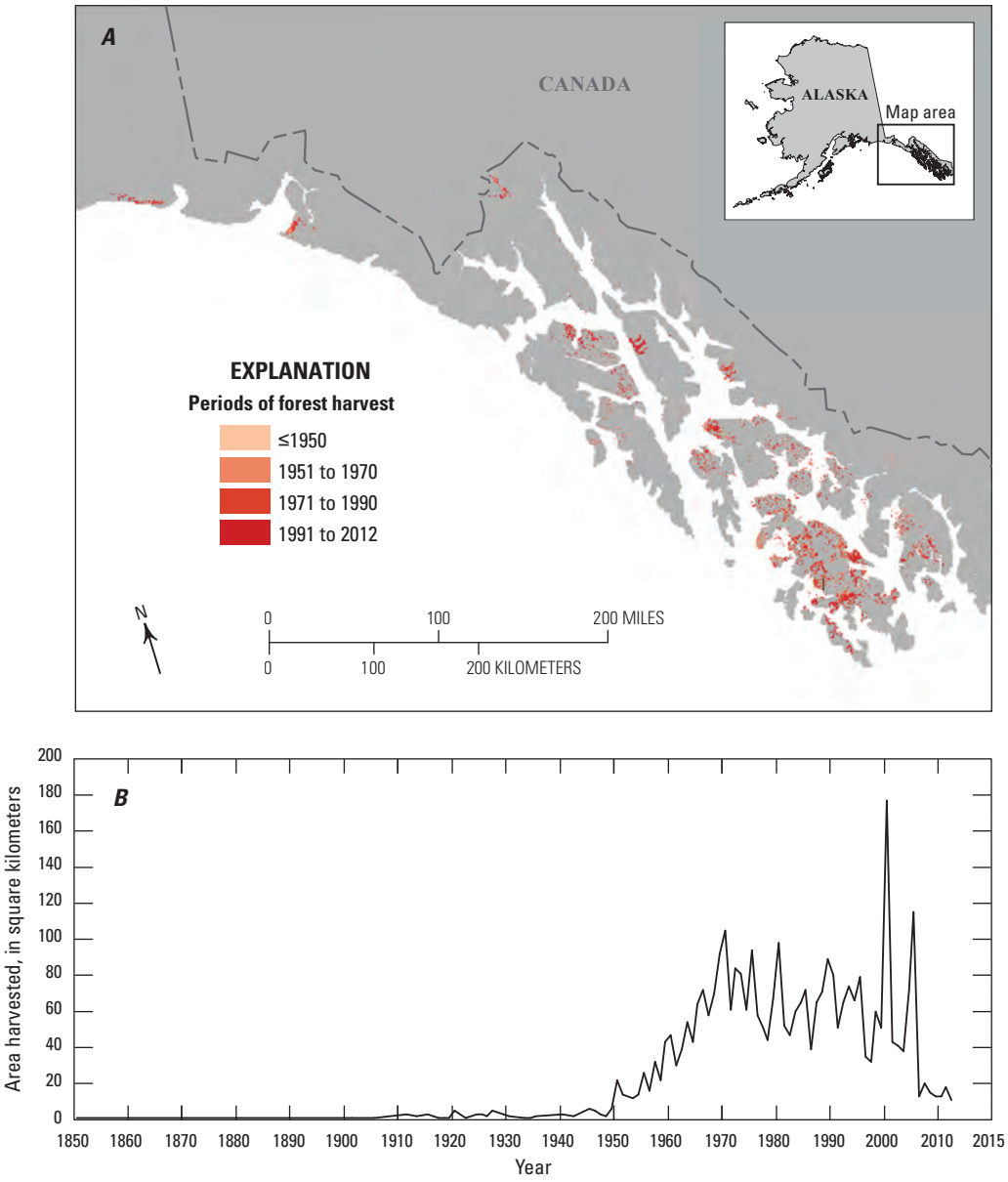

Figure 6.2. Forest harvest history in southeast and south-central Alaska: *A*, spatial distribution of harvests from 1850 through 2012 and *B*, time series of annual area harvested from 1850 through 2012.

data collected in the Bonanza Creek Long Term Ecological Research (LTER) program (Yuan and others, 2012). For the tundra communities, we used data collected at the Toolik Field Station (Shaver and Chapin, 1991; Van Wijk and others, 2003; Sullivan and others, 2007; Euskirchen and others, 2012; Gough and others, 2012; Sistla and others, 2013). Finally, for the maritime upland forest, we used data summarized in chapter 4, collected from a long-term carbon flux study in the North American Carbon Program (D'Amore and others, 2012). The target values for maritime alder shrubland were assessed from Binkley (1982). Target values of vegetation biomass, soil carbon pools, net primary productivity, and gross primary productivity for each upland land-cover type are described in table 6.1.

6.3.4.2. Methane Dynamics Module of the Terrestrial Ecosystem Model (MDM-TEM)

The upland simulation of MDM-TEM was parameterized using CH_4 measurements and key soil and climate factors made at three upland field sites—boreal forest at Bonanza Creek (B-F), tundra at the North Slope of Alaska (Tundra-NS), and moist tundra on Unalaska Island (Tundra-UI) (table 6.2). Because daily time series of CH_4 consumption were not available, we parameterized the MDM-TEM for upland ecosystems such that the difference between the simulated and observed maximum daily CH_4 consumption rate is minimized at these sites. Specifically, we altered the parameters of the methane module until the simulation CH_4 consumption

Table 6.1. Target values for carbon pool and flux variables used to calibrate the Dynamic Organic Soil version of the Terrestrial Ecosystem Model (DOS-TEM) for major upland land-cover types in Alaska.

[$gC/m^2/yr$, gram of carbon per square meter per year; gC/m^2, gram of carbon per square meter]

Upland land-cover type	Net primary productivity ($gC/m^2/yr$)	Gross primary productivity ($gC/m^2/yr$)	Carbon pool (gC/m^2)			
			Vegetation	Soil fibric	Soil humic	Soil mineral[1]
Boreal upland black spruce forest	186	372	6,405	1,199	4,432	19,821
Boreal upland white spruce forest	305	610	9,000	1,156	4,254	11,005
Boreal upland deciduous forest	510	1,020	8,546	996	3,597	11,005
Shrub tundra	136	272	1,808	2,340	5,853	37,022
Graminoid tundra	112	224	561	3,079	7,703	43,403
Heath tundra	23	46	249	1,065	1,071	32,640
Maritime upland forest	375	750	809	825	2,912	23,232
Maritime alder shrubland	300	600	24,290	2,557	4,136	15,564

[1]Soil mineral carbon pools are estimated from the bottom of the organic layer down to 1 meter into the mineral soil.

Table 6.2. Description of sites used in the model parameterization and validation process.

[n.d., no data]

Site name	Location	Elevation (meters)	Land cover	Observed data
Boreal forest at Bonanza Creek (B-F)	148°15' W. 64°41' N.	133	Black spruce (*Picea mariana*), feather moss (*Hylocomium splendens*)	Methane fluxes from late May through September 1990
Tundra at North Slope of Alaska (Tundra-NS)	149°36' W. 68°38' N.	760	Sedge (Carex spp.), moss tussock tundra dominated by *Eriophorum vaginatum*	Static chamber measured methane uptake
Moist tundra on Unalaska Island (Tundra-UI)	167°00' W. 53°00' N.	n.d.	Wet tundra dominated by sedges (Carex spp.)	Static chamber measured methane uptake
Tundra at Fairbanks, Alaska (Tundra-F; validation site)	147°51' W. 64°52' N.	158.5	Tussock tundra dominated by *Eriophorum vaginatum*	Three sites of methane emissions observed using chamber techniques from 1987 to 1990

by soil reached the maximum consumption rates of 31.6 milligrams of carbon dioxide equivalent per square meter per day ($mgCO_2$-eq/m^2/d), 39.9 $mgCO_2$-eq/m^2/d, and 56.5 $mgCO_2$-eq/m^2/d at the B-F, Tundra-NS, and Tundra-UI sites, respectively (Zhuang and others, 2004).

6.3.4.3. Model Validation and Verification

We validated the model by testing the ability of the model to extrapolate carbon dynamics across space and time. We compared model simulations with observations collected outside the spatial and temporal range of the data used for model parameterization and calibration. When independent observations were not available, we tested the ability of the model to reproduce the same data used for parameterization and calibration.

DOS-TEM parameterization has been validated using soil and vegetation biomass data derived from field observations independent of the data used for model parameterization. The National Soil Carbon Network database for Alaska was used to validate DOS-TEM estimates of soil carbon stocks (Johnson and others, 2011). In order to compare similar estimates from the model and observations, only deep profiles were selected from the database—that is, profiles with a description of the entire organic layer and the 90- to 110-centimeter (cm)-thick mineral layer below the organic layer.

Estimates of vegetation carbon stocks for tundra land-cover types were compared with observations recorded in the data catalog of the Arctic LTER at Toolik Field Station (http://toolik.alaska.edu; Shaver and Chapin, 1986). For boreal forest land-cover types, vegetation carbon stocks simulated by

DOS-TEM were compared with estimates from forest inventories conducted by the Cooperative Alaska Forest Inventory (Malone and others, 2009). The forest inventory only provided estimates of aboveground biomass. Aboveground biomass was converted to total biomass by using a ratio of aboveground versus total biomass of 0.8 in forest (Ruess and others, 1996) and 0.6 in tundra land-cover types (Gough and Hobbie, 2003). Carbon content of the biomass was estimated at 50 percent.

Finally, for the land-cover types of southern coastal Alaska (that is, the North Pacific Landscape Conservation Cooperative (LCC) maritime upland and wetland forests and maritime fen), model validation was not possible as no additional independent data were available in this region. For these land-cover types, we compared the model simulations with observed data on the same sites that were used for model parameterization. (See chapter 4, section 4.3.1 for site descriptions).

For MDM-TEM, the model was validated at a tundra site (Tundra-F) at Fairbanks, Alaska, which was not used during the parameterization process (table 6.2). The simulated daily CH_4 fluxes were compared to the observations. The Tundra-NS parameterization was used for the Tundra-F site simulations.

6.3.5. Model Application and Analysis

6.3.5.1. Forcing Data

The distribution of uplands in Alaska was assessed from topographic information. Uplands in Alaska are estimated to cover 1,237,775 square kilometers (km^2), which represents about 84 percent of the total Alaska lands (see chapter 7, section 7.4.1). Simulations were conducted across Alaska at a 1-km resolution from 1950 through 2099. DOS-TEM is driven by monthly mean air temperature, total precipitation, net incoming shortwave radiation, and vapor pressure. To evaluate the effects of historical and projected climate warming, a series of six climate simulations was conducted. The simulations combined (1) historical climate variability from 1901 through 2009 using Climatic Research Unit (CRU TS v. 3.10.01; Harris and others, 2014) data and (2) climate variability from 2010 through 2099 projected by version 3.1-T47 of the Coupled Global Climate Model (CGCM3.1, www.cccma.ec.gc.ca/data/cgcm3/; McFarlane and others, 1992; Flato, 2005) developed by the Canadian Centre for Climate Modelling and Analysis and version 5 of the European Centre Hamburg Model (ECHAM5, www.mpimet.mpg.de/en/wissenschaft/modelle/echam/; Roeckner and others 2003, 2004) developed by the Max Planck Institute. The climate projections were aligned with the Intergovernmental Panel on Climate Change's Special Report on Emissions Scenarios (IPCC-SRES; Nakićenović and Swart, 2000). The assessment used three low-, mid- and high-range CO_2 emissions scenarios (B1, A1B, and A2; see further details in chapter 2, section 2.2.1.). The climate data were bias corrected and downscaled using the delta method (Hay and others, 2000; Hayhoe, 2010) by the Scenarios Network for Alaska and Arctic Planning (SNAP, www.snap.uaf.edu/) from 0.5-degree original resolution data to 1-km resolution. The fire occurrence dataset combined (1) historical records from 1950 through 2009 obtained from the Alaska Interagency Coordination Center (AICC) large fire scar database (http://fire.ak.blm.gov/; see Kasischke and others, 2002) and (2) projected scenarios from ALFRESCO (see chapter 2, section 2.4.5.). These scenarios represent the changes in fire frequency in response to climate change and changes in vegetation composition over time. Topographic information used to compute fire severity was computed from the National Elevation Dataset of the U.S. Geological Survey at 60-meter (m) resolution (NED, http://ned.usgs.gov/). The topographic descriptors included slope, aspect, and log-transformed flow accumulation. Finally, soil texture information originated from the Global Gridded Surfaces of Selected Soil Characteristics dataset (Global Soil Data Task Group, 2000).

Historical records of area harvested from 1950 through 2009 in southeast and south-central Alaska were compiled combining geographic information system (GIS) data from four different sources: (1) The USDA Forest Service, Tongass National Forest; (2) The Nature Conservancy's past harvest repository; (3) three layers obtained from the State of Alaska—one covering Cape Yakataga to Icy Bay harvests, one for southeast Alaska, and one for Haines State Forest harvests; and (4) screen digitizing from high-resolution orthophotos of some harvests not included in the previously listed sources. In addition, the first three sources were edited using high-resolution orthophotos to improve some of the boundary delineations. Second-growth stands owing to forest harvest account for about 3.8 percent of southeast Alaska. We were unable to obtain reliable forest harvest data for areas west of Cape Yakataga and Icy Bay (that is, west of approximately long 142.55° W.). We used the harvest layer for two purposes: (1) to determine where forest harvest has taken place and (2) to identify second-growth areas on the landscape.

6.3.5.2. Analysis of Changes in Carbon Stocks and Climate-Related Uncertainty

Vegetation carbon stock estimates were derived from the sum of the aboveground and belowground living biomass. Soil carbon stocks were composed of carbon stored in the dead woody debris fallen to the ground, moss and litter, organic layers, and mineral layers. Historical changes in soil and vegetation carbon stocks were evaluated by quantifying annual differences of decadal averages between the first decade (1950–1959) and the last decade (2000–2009) of the historical period. Projected changes in soil and vegetation carbon stocks were evaluated by quantifying annual differences of decadal averages between the last decade of the historical period (2000–2009) and the last decade of the projection period (2090–2099).

The net ecosystem carbon balance (NECB) is the difference between total carbon inputs and total carbon outputs to the ecosystem (Chapin and others, 2006). NECB is the sum of all carbon fluxes coming in and out of the ecosystems, through gaseous and nongaseous, dissolved and nondissolved exchanges with the atmosphere and the hydrologic network. This chapter and chapter 7 report the carbon exchange between the terrestrial ecosystem and the atmosphere. Chapter 8 will consider carbon exchanges in inland aquatic ecosystems (gaseous and nongaseous). In terrestrial ecosystems, NECB is the result of net primary productivity (NPP) and net biogenic methane flux ($BioCH_4$) minus heterotrophic respiration (HR), fire emissions (Fire), and forest harvest exports (Harvest).

$$NECB = NPP + BioCH_4 - HR - Fire - Harvest \quad (6.1)$$

NPP results from carbon assimilation from vegetation photosynthesis minus the respiration of the primary producers (autotrophic respiration). In uplands, the activity of soil methanotrophs offset the activity of methanogens. For this reason, $BioCH_4$ is a positive flux in uplands. HR results from the decomposition of unfrozen soil organic carbon. Fire emissions encompass CO_2, CH_4, and carbon monoxide (CO) emissions. Forest harvest quantifies the amount of vegetation carbon that is exported out of the terrestrial ecosystem in the form of timber. For the analysis of the inter-annual variations in sections 6.4.1.2 and 6.4.2.1, carbon fluxes were expressed in grams of carbon per square meter per year ($gC/m^2/yr$). For the regional assessments in sections 6.4.1.4 and 6.4.2.3, carbon fluxes were summed across the regions and expressed in teragrams of carbon per year (TgC/yr). Positive NECB indicates a gain of carbon to the ecosystem from the atmosphere, and negative NECB indicates a loss of carbon from the ecosystem to the atmosphere.

The uncertainty of carbon dynamics projected through the 21st century associated with climate forcing was estimated spatially by computing the range of change in NECB among the six climate simulations. For every 1-km grid cell and every climate scenario, the annual change in NECB was computed as the difference in the mean decadal NECB centered on 2095 and 2005 divided by the length of this period:

$$\Delta NECB = \frac{(NECB_{[2090-2099]} - NECB_{[2000-2009]})}{90} \quad (6.2)$$

The uncertainty was computed as the difference between the maximum and minimum ΔNECB among the six climate simulations.

Global warming potential (GWP) across time and the landscape was estimated taking into consideration that CH_4 has 25 times the GWP of CO_2 over a 100-year timeframe (Forster and others, 2007). GWP values were reported in CO_2 equivalent after first converting C-CH_4 fluxes to CH_4 equivalent by multiplying the fluxes by 16/12, the ratio of the molecular weight of CH_4 to the weight of carbon in CH_4, and then converting CH_4 equivalent fluxes to CO_2 equivalent by multiplying by 25. All C-CO_2 fluxes were converted to CO_2 equivalent by multiplying them by 44/12, the ratio of the molecular weight of CO_2 to the weight of carbon in CO_2. CH_4 production from fire emissions ($Fire_{(CH4)}$) was considered in addition to soil CH_4 uptake and emissions by applying emission factors among CO_2, CH_4, and CO on DOS-TEM simulations of fire emissions (French and others, 2002). The carbon in CO was considered CO_2 because it converts to CO_2 in the atmosphere within a year (Weinstock, 1969).

$$GWP = -44/12 \times (NPP - HR - Harvest - Fire_{(CO2+CO)}) + 25 \times 16/12 \times (Fire_{(CH4)} - BioCH_4) \quad (6.3)$$

Positive GWP indicates net CO_2 loss from the ecosystem to the atmosphere, and negative GWP indicates net CO_2 gain to the ecosystem from the atmosphere.

Analysis of the time series was conducted using linear regression and the Fisher test for test of significance on the time series. For the analysis of the inter-annual variations in sections 6.4.1.2 and 6.4.2.1, carbon fluxes were expressed in $gC/m^2/yr$ with associated standard deviation (s.d.). For the regional assessments in sections 6.4.1.4 and 6.4.2.3, carbon fluxes were summed across the regions and expressed in TgC/yr. The assumptions of normality and homoscedasticity were verified by examining residual plots. The relative effects of temperature, precipitation, total area burned, and atmospheric CO_2 concentration on the carbon fluxes were tested using multiple regression analysis. The effects were considered significant when the p-value is lower than 0.05.

6.4. Results and Discussion

6.4.1. Historical Assessment of Carbon Dynamics (1950–2009)

6.4.1.1. Model Validation and Verification

For the historical period of the simulations (1950–2009), soil and vegetation carbon stocks were validated when possible by comparing modeled and observed estimates at sites independent from the sites used for model parameterization. When independent data (that is, data collected outside of the sites used for model parameterization) were not available, a verification of modeled versus observed stocks was conducted on the same sites used for model parameterization.

Globally, no significant differences were observed between modeled and observed contemporary vegetation carbon stocks (table 6.3; p-value, $p=0.340$) and soil carbon stocks (table 6.4; $p=0.085$). In general, DOS-TEM simulations successfully reproduced differences between land-cover types. Arctic or alpine tundra and shrubland presented the lowest vegetation carbon stocks (table 6.3). Boreal land-cover types had intermediate vegetation carbon stocks and maritime upland forest presented the largest vegetation carbon stocks, with 19.3 kilograms of carbon per square meter (kgC/m^2) observed.

In contrast, arctic and alpine tundra and shrublands presented larger soil carbon stocks than boreal forests and maritime upland forest (table 6.4).

Table 6.3. Comparison of observed and modeled vegetation carbon stocks for the main upland land-cover types in Alaska.

[kgC/m^2, kilogram of carbon per square meter; NA, not applicable]

Land-cover type	Number of sites used for model testing	Vegetation carbon stocks (kgC/m^2)			
		Mean		Standard deviation	
		Observed	Modeled	Observed	Modeled
Black spruce forest	45	2.47	1.99	0.85	0.38
White spruce forest	20	4.40	4.29	0.74	0.32
Deciduous forest	24	6.85	6.56	0.46	0.85
Shrub tundra	4	1.81	2.26	0.12	0.50
Tussock tundra	3	0.56	0.44	0.26	0.21
Wet-sedge tundra	2	0.46	0.83	0.17	0.32
Heath tundra[1]	1	0.25	0.32	NA	NA
Maritime upland forest[1]	3	19.26	22.10	3.79	4.56
Maritime alder shrubland[1]	1	0.81	0.96	NA	NA

[1]Comparisons between observed and modeled vegetation carbon stocks have been conducted for parameterization (that is, verification).

Table 6.4. Comparison of observed and modeled soil carbon stocks for the main upland land-cover types in Alaska.

[kgC/m^2, kilogram of carbon per square meter; NA, not applicable]

Land-cover type	Number of sites used for model testing	Soil carbon stocks (kgC/m^2)			
		Mean		Standard deviation	
		Observed	Modeled	Observed	Modeled
Black spruce forest	40	29.85	46.84	11.15	55.64
White spruce forest	32	23.05	25.18	9.61	54.08
Deciduous forest	65	23.87	22.10	12.96	29.83
Shrub tundra	66	36.73	44.14	19.11	77.93
Tussock tundra	11	62.53	65.44	20.83	49.59
Wet-sedge tundra	23	42.01	50.73	30.49	31.46
Heath tundra	5	34.78	32.71	20.41	38.38
Maritime upland forest[1]	1	15.05	23.89	NA	NA
Maritime alder shrubland[1]	1	26.97	23.55	NA	NA

[1]Comparisons between observed and modeled soil carbon stocks have been conducted for parameterization (that is, verification).

6.4.1.2. Times Series for Upland Alaska

From 1950 to 2000, the long-term trend of vegetation carbon stocks in uplands increased slightly owing to an increase in NPP (fig. 6.3*A*). The increase of NPP (0.185 $gC/m^2/yr$, s.d. 0.254 $gC/m^2/yr$ computed for the entire study area) across the entire historical period was significant (fig. 6.3*C*; Fisher value, F=17.15; p<0.001). However, large fire years in 1957, 1969, 1977, 1990 and 1991 (fig. 6.3*D*) caused sudden decreases of vegetation carbon stocks (by 37 grams of carbon per square meter [gC/m^2], 28 gC/m^2, 3 gC/m^2, and 22 gC/m^2, respectively) that slowed carbon accumulation over the period. The intense fire years of 2004 and 2005 caused the largest loss of vegetation carbon stocks of the historical period—by 80 gC/m^2 over the two consecutive years—shifting the vegetation net change over the historical period from a net carbon gain by 2000 to a net carbon loss by 2009. For the entire historical period, 2.09 $gC/m^2/yr$ of vegetation carbon stocks was exported out of the ecosystem by forest harvest activities (fig. 6.3*D*). By 2009, the vegetation across upland Alaska lost 35.9 gC/m^2 from 1950.

Soil carbon stocks in upland Alaska remained relatively stable from 1950 to the late 1970s (fig. 6.3*B*). The large fire years 1957, 1969, and 1977 induced a loss of soil carbon stocks of 35 gC/m^2, 21 gC/m^2, and 17 gC/m^2, respectively. From the early 1980s through 2009, soil carbon stocks increased mostly because of increases in litterfall associated with increases in NPP and the increase in dead woody debris produced during wildfire, which more than offset the increase of carbon loss from heterotrophic respiration (fig. 6.3*E*) and carbon emissions from wildfire (fig. 6.3*D*). CH_4 uptake by the methanotrophs in upland Alaska is quite low (fig. 6.3*F*), ranging from 3.43 to 6.35 milligrams of carbon dioxide equivalent per square meter per year. The MDM-TEM simulation estimates Alaskan uplands to be a net sink of CH_4. Overall, soils across upland Alaska accumulated carbon throughout the historical period, increasing by 159 gC/m^2 from 1950 through 2009.

The mean NECB throughout the historical period was estimated at 1.66 $gC/m^2/yr$ (s.d. 3.82 $gC/m^2/yr$ computed amongst all five LCC regions; fig. 6.3*G*). Carbon gain to the ecosystem was mainly composed of net primary productivity, CH_4 uptake being negligible. Carbon loss from the ecosystem was composed of heterotrophic respiration (93.6 percent), wildfire emissions (4.7 percent), and forest harvest exports (1.6 percent). Despite the larger CH_4 emissions from fire compared to CH_4 uptake by methanotrophs, upland Alaska was on average a carbon sink through the historical period of –13.3 grams of carbon dioxide equivalent per square meter per year (gCO_2-$eq/m^2/yr$) (s.d. 33.8 gCO_2-$eq/m^2/yr$ computed amongst all five LCC regions; fig. 6.3*H*).

6.4.1.3. Environmental Drivers of the Temporal Variability of Net Ecosystem Carbon Balance in Upland Alaska

During the historical period, NPP was influenced primarily by mean annual temperature (table 6.5). Heterotrophic respiration increased during dry and warm years and large fire years. The positive relationship between heterotrophic respiration and large fire years might be related to (1) permafrost thaw in burned soils and (2) large inputs of carbon to the soil from the dead belowground vegetation biomass. Not surprisingly, fire emissions were driven

Table 6.5. Results of multiple linear regressions testing the main drivers of carbon dioxide and methane fluxes in upland ecosystems among the total annual precipitation, mean annual temperature, annual area burned, and mean annual atmospheric carbon dioxide (CO_2) concentration for the entire study area during the historical period (1950–2009).

[F, Fisher value; P, probability value. Trend: +, positive; –, negative; n.s., trend not significant. Units: mm, milllimeter; °C, degree Celsius; km^2, square kilometer; ppm, part per million]

Driver of carbon dioxide and methane fluxes	Net primary productivity			Heterotrophic respiration			Fire emissions			Methane uptake			Net ecosystem carbon balance		
	F	P	Trend	F	P	Trend	F	P	Trend	F	P	Trend	F	P	Trend
Total annual precipitation (mm)	3.37	0.07	n.s.	8.74	<0.01	–	0.02	0.89	n.s.	0.01	0.93	n.s.	0.94	0.34	n.s.
Mean annual temperature (°C)	14.29	0.00	+	5.78	0.02	+	1.18	0.28	n.s.	31.96	<0.01	+	0.33	0.57	n.s.
Annual area burned (km^2)	3.04	0.09	n.s.	10.29	<0.01	+	252.4	<0.01	+	19.59	<0.01	+	154.85	<0.01	–
Mean annual atmospheric CO_2 concentration (ppm)	1.83	0.07	n.s.	3.72	0.06	n.s.	1.29	0.26	n.s.	0.26	0.61	n.s.	7.43	0.01	+

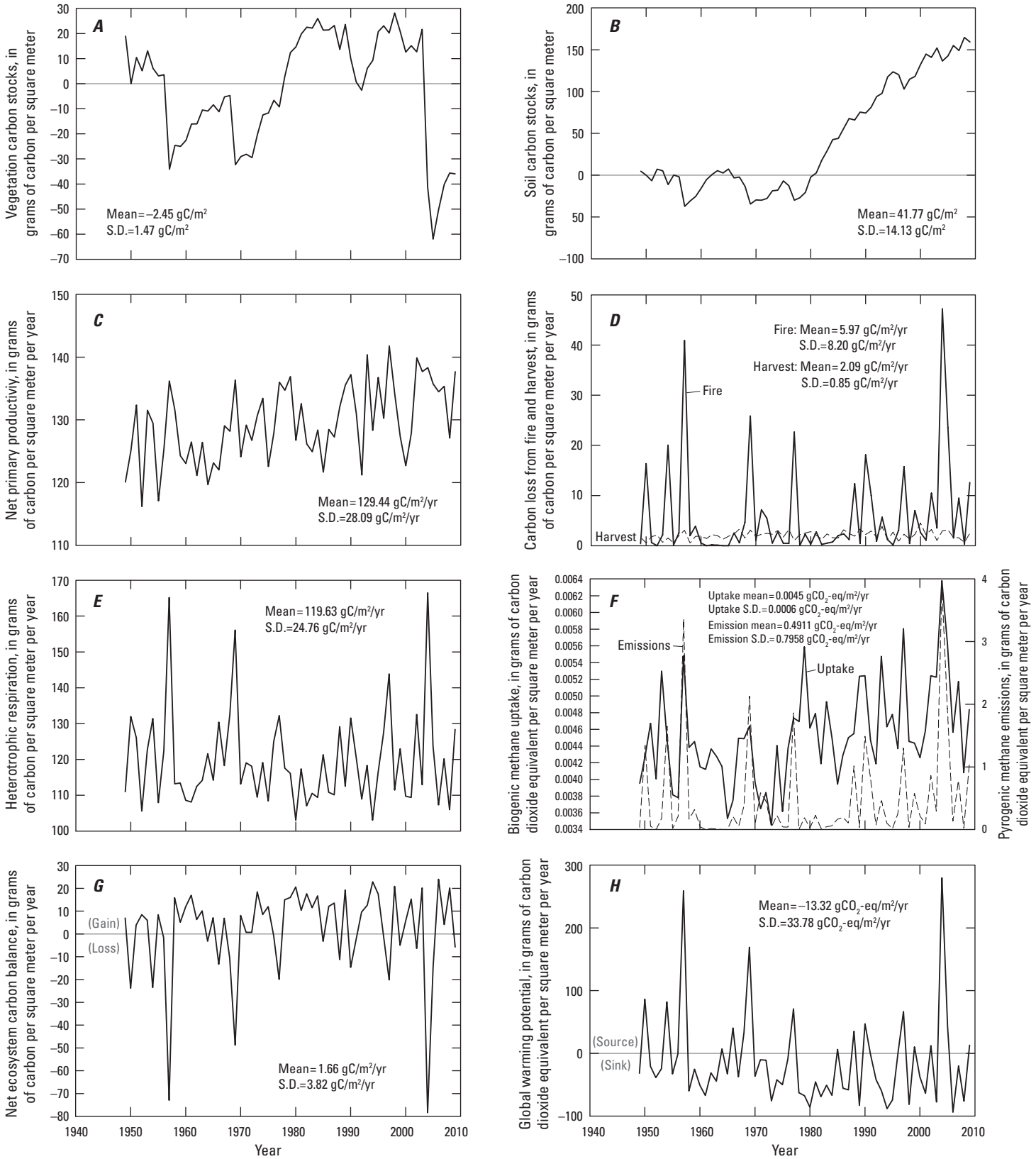

Figure 6.3. Time series of relative changes in carbon stocks and fluxes through the historical period (1950–2009). *A*, vegetation carbon stocks. *B*, soil carbon stocks. *C*, net primary productivity carbon flux. *D*, carbon loss from fire emissions and forest harvest exports. *E*, soil heterotrophic respiration. *F*, biogenic methane uptake and pyrogenic methane emissions. *G*, net ecosystem carbon balance. *H*, global warming potential. Mean and standard deviations for the entire study area are indicated in each panel.

primarily by large fire years. CH_4 uptake was positively correlated to air temperature and large fire years, perhaps because of the influence of fire on soil temperature. Finally, the primary drivers of the temporal variability of NECB were the fire activity and the atmospheric CO_2 concentration. The lack of effect of mean annual temperature on NECB was related to the fact that temperature had a positive effect on NPP and CH_4 uptake, which was offset by its positive effect on heterotrophic respiration.

6.4.1.4. Spatial Distribution of Net Ecosystem Carbon Balance Across Upland Alaska

The largest upland vegetation carbon stocks for the historical period are located in the Northwest Boreal LCC North and North Pacific LCC, whereas the largest soil carbon stocks are located in the Arctic and Western Alaska LCCs (table 6.6). Vegetation carbon storage decreased during the historical period in the regions that represent the largest vegetation carbon stocks: the Northwest Boreal LCC North and North Pacific LCC. The decrease of vegetation carbon stocks in the Northwest Boreal LCC North is related to carbon loss from fire. Carbon exports associated with forest harvest disturbance induced a decrease of vegetation carbon stocks in the North Pacific LCC (tables 6.6 and 6.7; chapter 5, section 5.5). The largest NPP and HR values were found in the two largest ecoregions (Northwest Boreal LCC North and Western Alaska LCC). The Northwest Boreal LCC North and Western Alaska LCC were the two major contributors to the regional total upland CH_4 uptake, together contributing more than 70 percent of the total regional uptake, followed by the Northwest Boreal LCC South and Arctic LCC, which each contributed around 10 percent of the total. Whereas loss of vegetation carbon stocks in the North Pacific LCC was offset

Table 6.6. Average vegetation and soil carbon stocks from the last decade (2000–2009) of the historical period and mean annual change in vegetation and soil carbon stocks between the first (1950–1959) and the last (2000–2009) decades of the historical period in each Landscape Conservation Cooperative region.

[Data may not add to totals shown because of independent rounding. TgC, teragram of carbon; km², square kilometer]

Landscape Conservation Cooperative (LCC) region	Upland total area (km²)	Upland cover (percent)	Vegetation carbon stocks (TgC)		Soil carbon stocks (TgC)	
			Average	Mean annual change	Average	Mean annual change
Arctic LCC	261,481	86	344	0.77	10,864	2.41
Western Alaska LCC	327,327	88	1,054	0.66	17,790	3.13
Northwest Boreal LCC North	335,491	73	1,272	–1.75	6,686	–3.37
Northwest Boreal LCC South	163,388	88	505	0.15	6,975	0.41
North Pacific LCC	150,087	97	1,119	–0.10	4,799	2.69
Total	**1,237,774**	**84**	**4,293**	**–0.26**	**47,113**	**5.27**

Table 6.7. Average vegetation and soil carbon fluxes in upland ecosystems per Landscape Conservation Cooperative region from 2000 through 2009.

[Data may not add to totals or compute to net ecosystem carbon balance shown because of independent rounding. CO, carbon monoxide; CO_2, carbon dioxide; TgC/yr, teragram of carbon per year; $TgCO_2$-eq/yr, teragram of carbon dioxide equivalent per year; NA, not applicable]

Landscape Conservation Cooperative (LCC) region	Fire emissions ($CO+CO_2$) (TgC/yr)	Pyrogenic methane emissions ($TgCO_2$-eq/yr)	Net primary productivity (TgC/yr)	Harvesting (TgC/yr)	Methane uptake ($TgCO_2$-eq/yr)	Heterotrophic respiration (TgC/yr)	Net ecosystem carbon balance (TgC/yr)	Global warming potential ($TgCO_2$-eq/yr)
Arctic LCC	2.47	0.26	32.14	NA	7.58×10^{-4}	26.48	3.18	–11.44
Western Alaska LCC	1.34	0.13	60.29	NA	1.74×10^{-3}	55.15	3.79	–13.78
Northwest Boreal LCC North	22.23	2.00	71.57	NA	2.89×10^{-3}	54.40	–5.12	20.57
Northwest Boreal LCC South	2.75	0.29	22.70	NA	7.61×10^{-4}	19.38	0.57	–1.82
North Pacific LCC	0.14	0.01	25.27	2.91	9.31×10^{-5}	19.62	2.59	–9.49
Total	**28.94**	**2.69**	**211.97**	**2.91**	$\mathbf{6.25\times10^{-3}}$	**175.03**	**5.01 (gain)**	**–15.96 (sink)**

by the increase in soil carbon stocks, resulting in a positive NECB (table 6.7), carbon loss from wildfire caused negative NECB in the Northwest Boreal LCC North, the largest ecoregion of Alaska. Statewide for the historical period, upland ecosystems were a carbon sink, gaining on average 5 TgC/yr. The Arctic and the North Pacific LCCs and southern portions of the Western Alaska LCC were hotspots of high carbon gain (blue shades in fig. 6.4*A*). Areas that lost carbon in Northwest Boreal LCC North mainly correspond to large historical fire scars (fig. 6.4*B*).

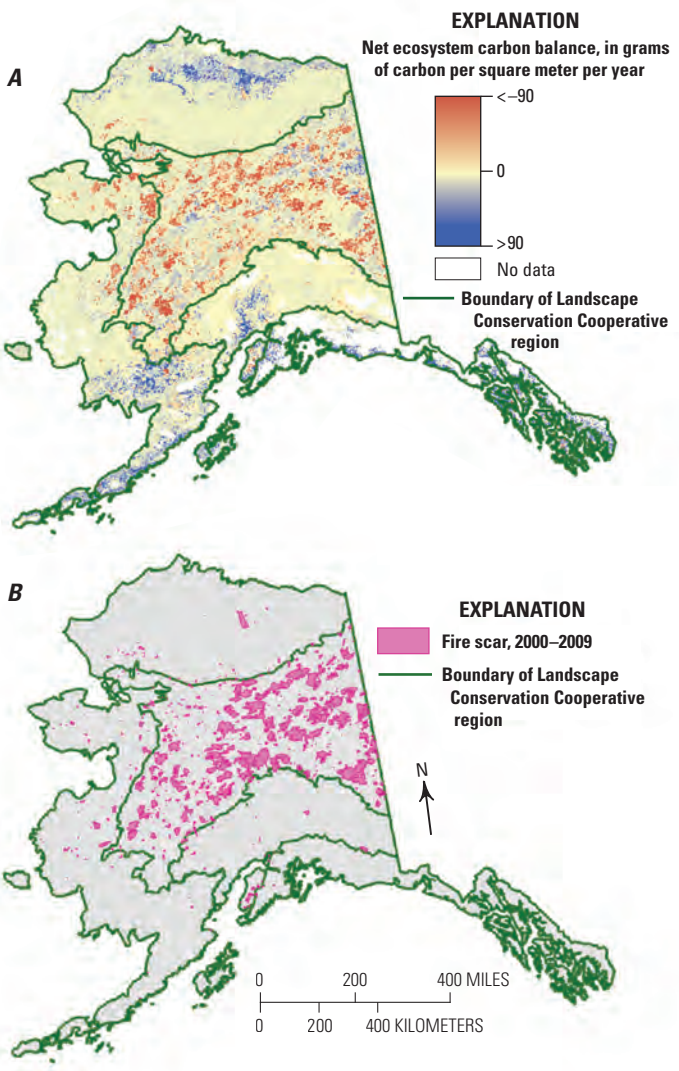

Figure 6.4. Spatial distribution of *A*, annual carbon loss and gain across upland Alaska during the historical period (1950–2009) and *B*, historical fire scars from 2000 through 2009 among the five Landscape Conservation Cooperative regions. See figure 7.2 for the distribution of uplands and wetlands in Alaska.

6.4.2. Assessment of Future Potential Carbon Dynamics (2010–2099)

6.4.2.1. Times Series for Upland Alaska

The carbon accumulation rate in vegetation was projected to increase over the 21st century for all climate simulations. The carbon accumulation rate was higher for the ECHAM5 simulations than for the CGCM3.1 simulations and higher for the highest CO_2 emissions scenarios (A2, followed by A1B and B1) (fig. 6.5*A*). From 2010 through 2099, the mean annual increase of vegetation carbon stocks would range from 310 gC/m^2/yr (under scenario B1 with CGCM3.1) to 579 gC/m^2/yr (under scenario A2 with ECHAM5). Carbon accumulation in the soil was quantitatively more important for the CGCM3.1 simulations than for the ECHAM5 simulations and higher for the higher CO_2 emissions scenarios (fig. 6.5*B*). From 2010 through 2099, the mean annual increase in soil carbon stocks would range from 296 gC/m^2/yr (under scenario A2 with ECHAM5) to 1,041 gC/m^2/yr (under scenario A2 with CGCM3.1). For all climate simulations, NPP and CH_4 uptake were projected to increase over the 21st century (figs. 6.5*C*, 6.5*F*), whereas heterotrophic respiration would not (fig. 6.5*E*). The projected increase in CH_4 uptake in the upland ecosystems is likely attributed to increasing microbial substrate availability as a result of increased vegetation productivity (van den Pol-van Dasselarr and others, 1998). Projected warming may also contribute to the enhanced metabolic activity of methanotroph microbes (Yonemura and others, 2000). The difference in magnitude of CH_4 uptake among emissions scenarios is generally greater than that between the GCMs. The A2 scenario has the highest projected increase in uptake, whereas the projected CH_4 uptake under scenario B1 does not differ significantly from the historical period, owing to the scenario's low anthropogenic CO_2 emissions. CH_4 emissions from wildfire would offset CH_4 uptake by methanotrophs in all climate scenarios (figs. 6.5*F*, 6.5*G*). The mean fire emissions for scenarios B1, A1B, and A2 were projected to be 9.7 gC/m^2/yr, 6.7 gC/m^2/yr, and 15.6 gC/m^2/yr for CGCM3.1 compared with 15.5 gC/m^2/yr, 17.0 gC/m^2/yr, and 18.2 gC/m^2/yr, respectively, for ECHAM5 simulations. CH_4 emissions represented 0.25 percent of the total projected carbon emissions from wildfire. The larger fire emissions associated with the ECHAM5 climate simulations compared with the CGCM3.1 simulations (fig. 6.5*D*) were mostly responsible for lower soil carbon accumulation with the ECHAM5 climate simulations compared with the CGCM3.1 simulations (fig. 6.5*B*).

The projected larger carbon accumulation in the ecosystem for the highest CO_2 emissions scenario was mostly related to the projected increase in ecosystem productivity in response to the fertilization effect of rising atmospheric CO_2

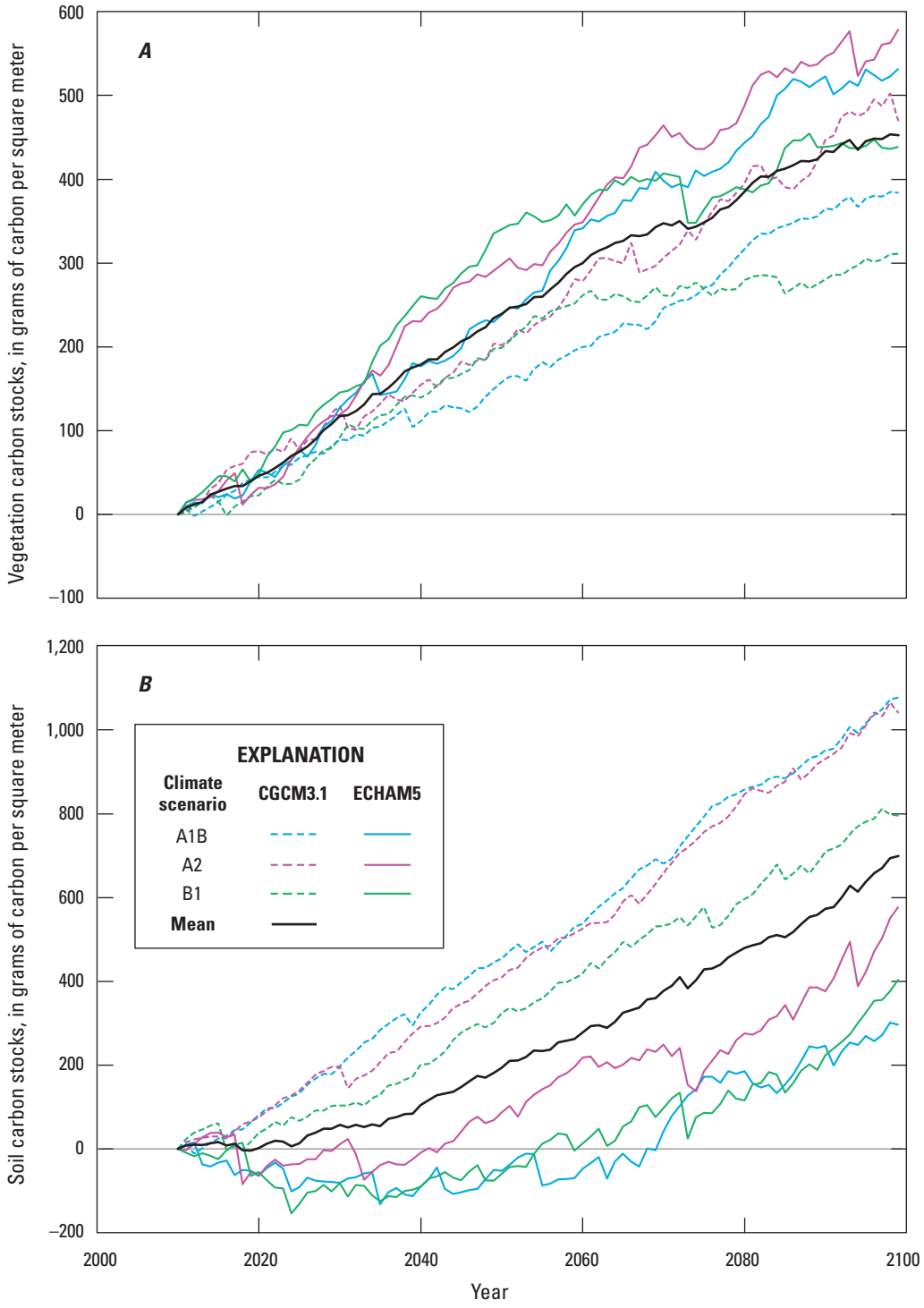

Figure 6.5 (pages 118–122). Time series of relative changes in carbon stocks and fluxes for the projection period (2010–2099) for the six climate simulations: *A*, vegetation carbon stocks; *B*, soil carbon stocks; *C*, net primary productivity; *D*, carbon loss from fire emissions; *E*, soil heterotrophic respiration; *F*, biogenic methane uptake; *G*, pyrogenic methane emissions; *H*, net ecosystem carbon balance; and *I*, global warming potential. Thick black lines represent annual averages amongst all six simulations. The six climate simulations are combinations of two general circulation models, version 3.1-T47 of the Coupled Global Climate Model (CGCM3.1) developed by the Canadian Centre for Climate Modelling and Analysis and version 5 of the European Centre Hamburg Model (ECHAM5) developed by the Max Planck Institute, and three climate scenarios of the Intergovernmental Panel on Climate Change's Special Report on Emissions Scenarios (Nakićenović and Swart, 2000), B1, A1B, and A2, in order of low to high projected CO_2 emissions.

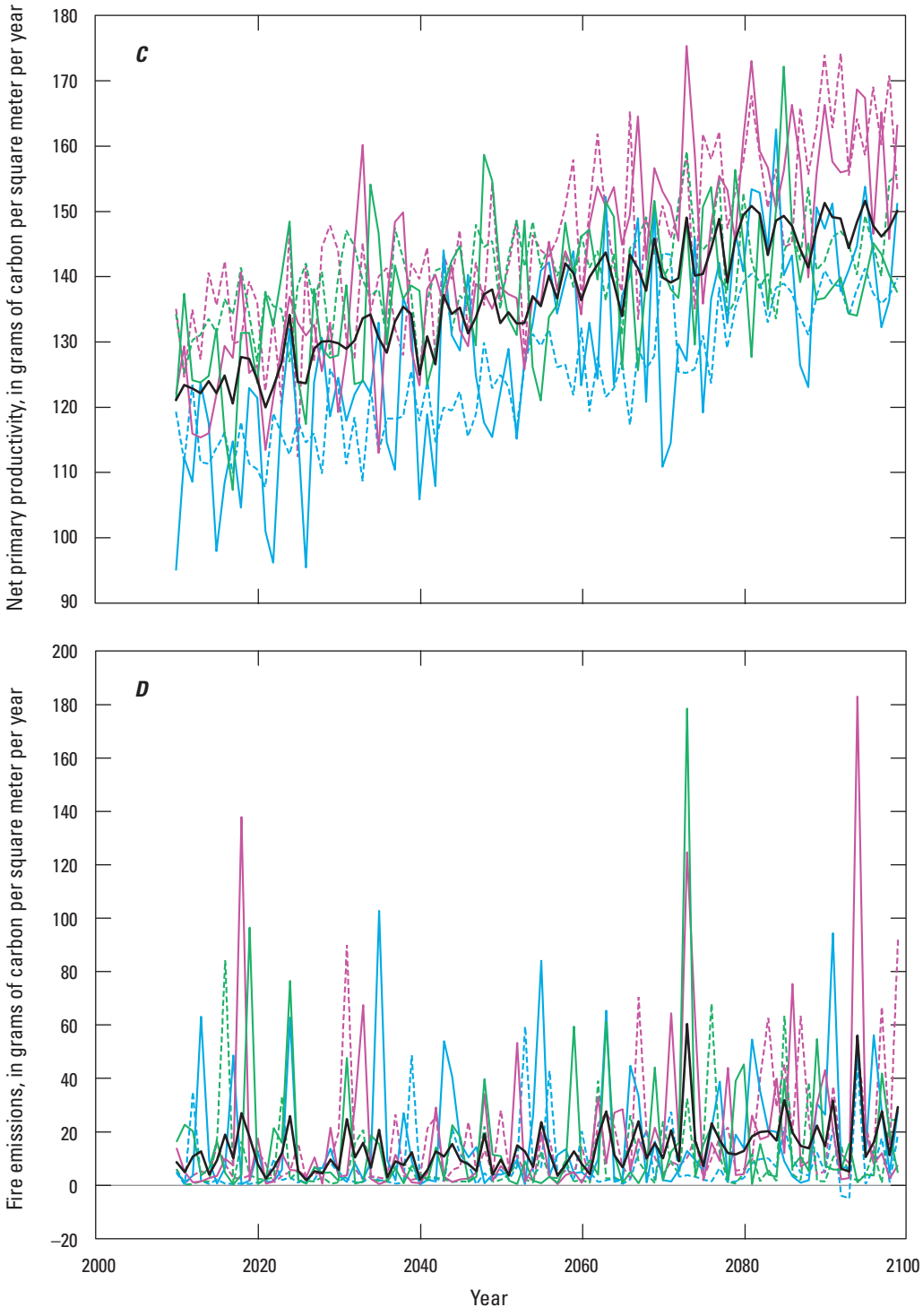

Figure 6.5.—Continued

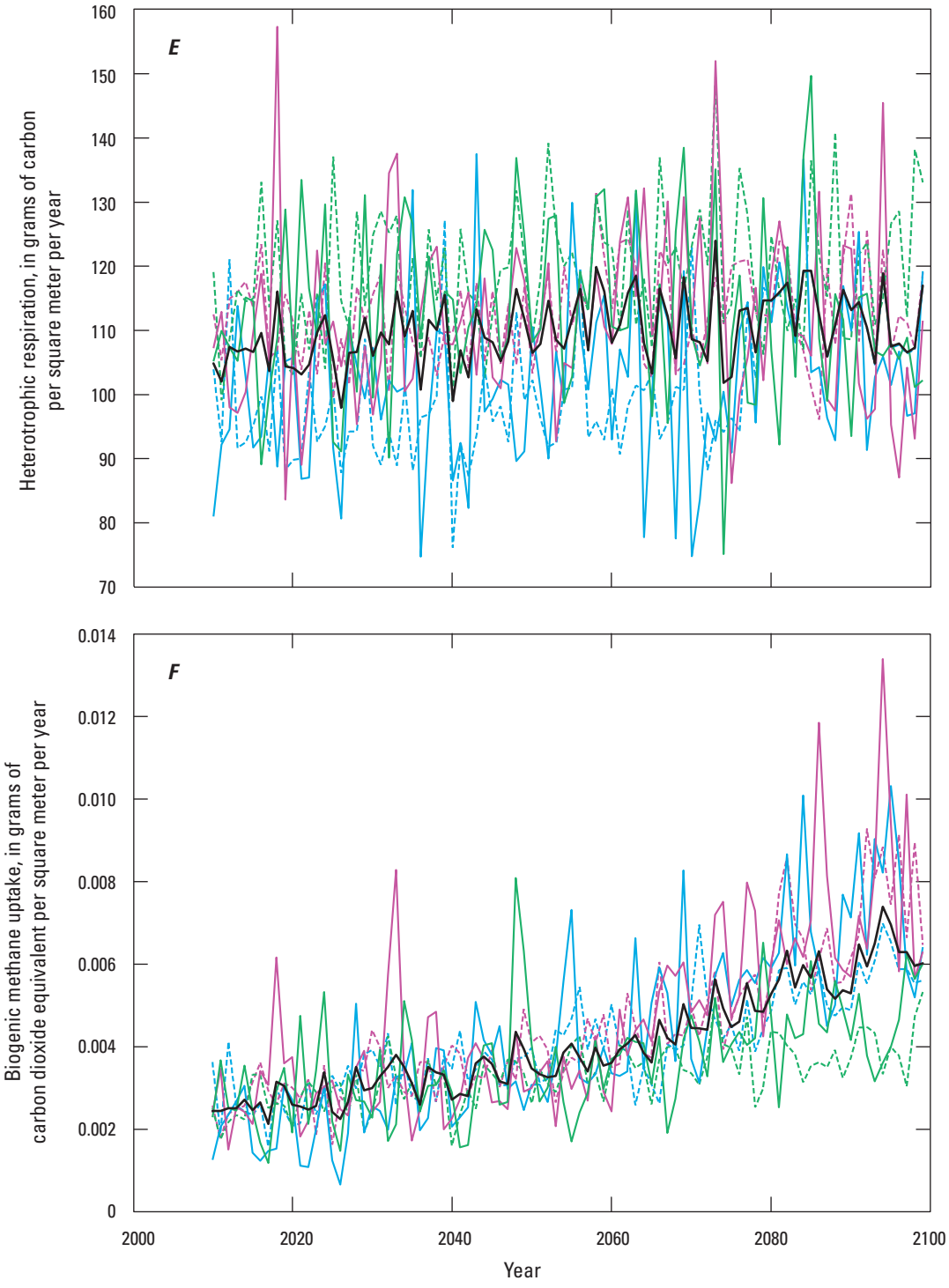

Figure 6.5.—Continued

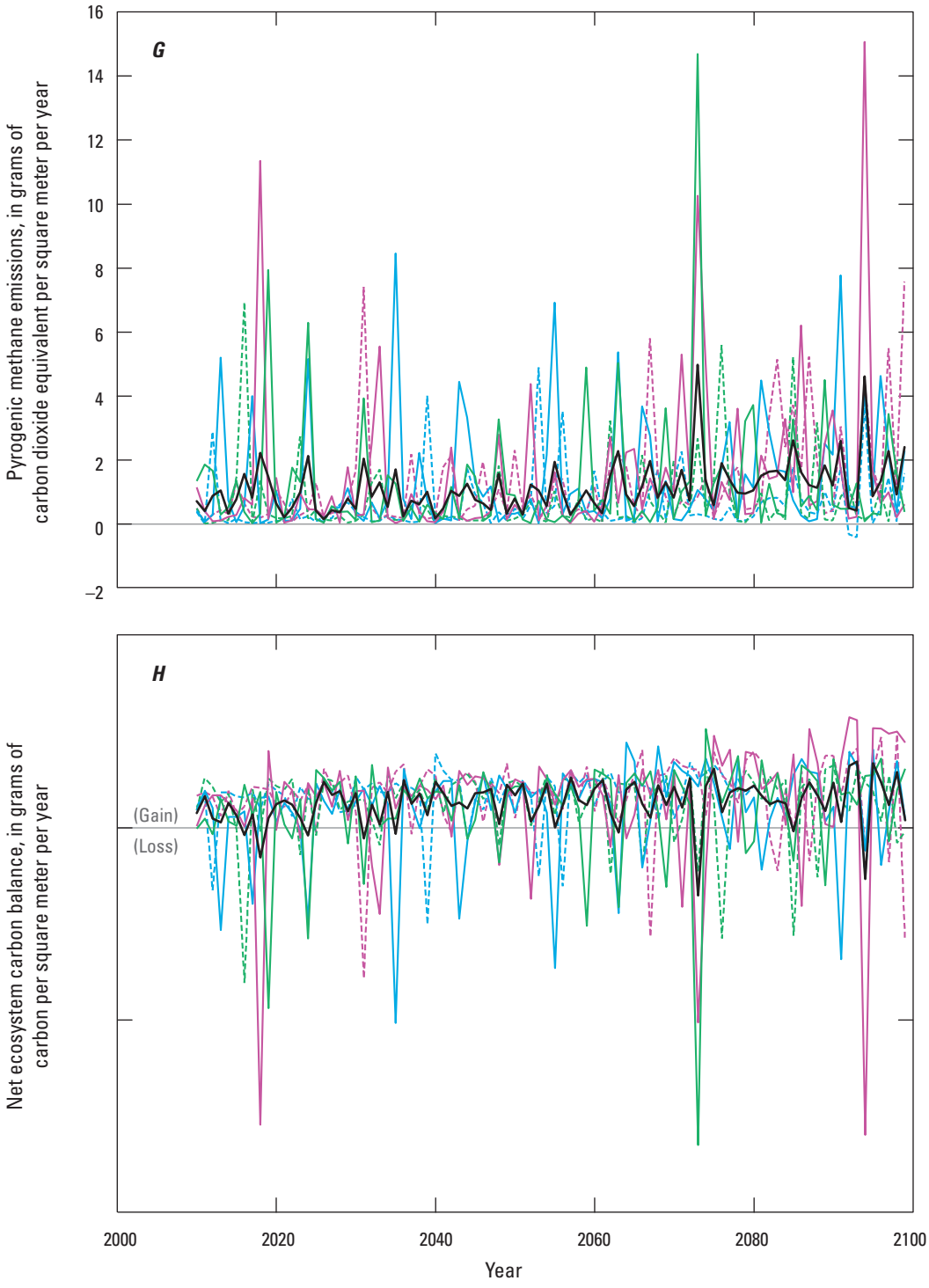

Figure 6.5.—Continued

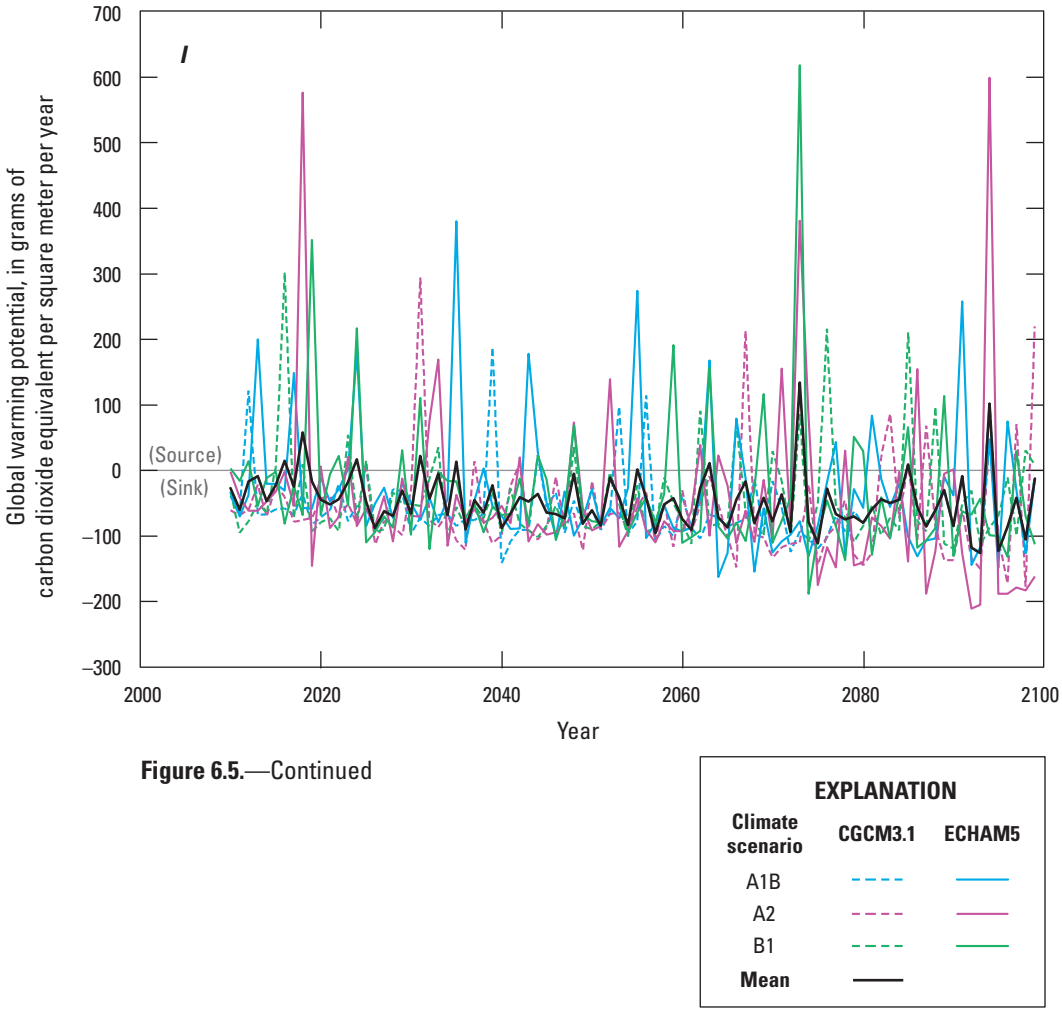

Figure 6.5.—Continued

concentration. NECB would increase during the 21st century for all scenarios (fig. 6.5*H*). However, this increase was only marginally significant because of the large inter-annual variability associated with large fire years (fig. 6.5*D*). On average, annual carbon gain in upland ecosystems in Alaska between 2010 and 2099 was projected to be 12.4 $gC/m^2/yr$, 17.1 $gC/m^2/yr$, and 17.0 $gC/m^2/yr$ for scenarios B1, A1B, and A2, respectively, with CGCM3.1 and 9.4 $gC/m^2/yr$, 9.3 $gC/m^2/yr$, and 12.9 $gC/m^2/yr$ for scenarios B1, A1B, and A2, respectively, with ECHAM5. Despite the large projected CH_4 emissions from wildfires, uplands in Alaska would be a CO_2 sink of –44.82 $gCO_2\text{-eq}/m^2/yr$, –61.12 $gCO_2\text{-eq}/m^2/yr$, and –62.2 $gCO_2\text{-eq}/m^2/yr$ for scenarios B1, A1B, and A2, respectively, with CGCM3.1 and –33.22 $gCO_2\text{-eq}/m^2/yr$, –32.82 $gCO_2\text{-eq}/m^2/yr$, and –45.8 $gCO_2\text{-eq}/m^2/yr$ for scenarios B1, A1B, and A2, respectively, with ECHAM5 for the same period.

6.4.2.2. Environmental Drivers of the Temporal Variability of Net Ecosystem Carbon Balance in Upland Alaska

Mean annual temperature was projected to positively control NPP and CH_4 uptake (table 6.8). Compared with similar analysis on the historical period, the present analysis across climate and CO_2 simulations projected a positive effect of atmospheric CO_2 concentration on NPP and CH_4 uptake, and as a result, NECB. Finally, annual area burned would influence heterotrophic respiration, fire emissions, and CH_4 uptake. As for the historical period, the positive effect of annual area burned on heterotrophic respiration and CH_4 uptake might be related to the effect of wildfire on soil temperature. The positive effect of area burned on heterotrophic respiration and fire emissions would cause a negative relationship between area burned and NECB.

Table 6.8. Results of multiple linear regressions testing the main drivers of carbon dioxide and methane fluxes in upland ecosystems among the total annual precipitation, mean annual temperature, annual area burned, and mean annual atmospheric carbon dioxide (CO_2) concentration for the entire study area during the projection period (2010–2099).

[F, Fisher value; P, probability value. Trend: +, positive; –, negative; n.s., trend not significant. Units: mm, milllimeter; °C, degree Celsius; km^2, square kilometer; ppm, part per million]

Driver of carbon dioxide and methane fluxes	Net primary productivity			Heterotrophic respiration			Fire emissions			Methane uptake			Net ecosystem carbon balance		
	F	P	Trend	F	P	Trend	F	P	Trend	F	P	Trend	F	P	Trend
Total annual precipitation (mm)	0.02	0.88	n.s.	1.69	0.19	n.s.	0.09	0.76	n.s.	3.89	0.05	n.s.	0.56	0.34	n.s.
Mean annual temperature (°C)	24.7	<0.01	+	2.61	0.11	n.s.	1.68	0.19	n.s.	89.4	<0.01	+	1.98	0.57	n.s.
Annual area burned (km^2)	1.68	0.19	n.s.	96.6	<0.01	+	1,144	<0.01	+	78.2	<0.01	+	997	<0.01	–
Mean annual atmospheric CO_2 concentration (ppm)	20.63	<0.01	+	0.72	0.39	n.s.	0.62	0.43	n.s.	85.2	<0.01	+	12.6	<0.01	+

6.4.2.3. Spatial Distribution of Net Ecosystem Carbon Balance Across Upland Alaska

Vegetation carbon stocks in uplands were projected to increase through the 21st century for the six climate simulations and all LCC regions of Alaska, except for the Northwest Boreal LCC South for the A1B and B1 scenarios with CGCM3.1. Statewide projected annual change in vegetation carbon stocks would range from 5.1 to 10.5 TgC/yr. As for the historical period, the largest vegetation carbon accumulation was projected for the North Pacific LCC and the Northwest Boreal LCC North (table 6.9). Soil carbon stocks would increase between 2000–2009 and 2090–2099 for all climate scenarios and LCC regions, except for ECHAM5 simulations in the Western Alaska LCC. In this region, precipitation was projected to increase the least, and some areas would likely experience some seasonal decreases in spring and summer (chapter 2, fig. 2.3). Drought stresses associated with these scenarios might decrease vegetation productivity in the Western Alaska LCC and also increase heterotrophic respiration and fire occurrence by decreasing soil moisture (table 6.10). Statewide, projected annual change in soil carbon stocks between 2000–2009 and 2090–2099 would range from 6.5 to 23.0 TgC/yr.

As a result, by the late 2090s, NECB would be positive for all LCC regions and climate simulations, ranging from 0.1 to 9.84 TgC/yr (table 6.10). Compared with the historical period, NECB would increase for each climate simulation, except for the ECHAM5 simulations in the Western Alaska LCC. Across Alaska, the increase in NPP associated with increasing air temperature would offset the carbon loss from increased wildfire and heterotrophic respiration.

The increase of NECB during the 21st century was higher for the model representing the lowest warming trend (CGCM3.1) compared with the model with the highest warming trend (ECHAM5). The negative relationship between change in NECB and warming was related to the effect of warming on wildfire regime that would offset the increase of vegetation productivity (table 6.11).

The spatial variability of the change in NECB over the 21st century was projected to be largest in the Northwest Boreal LCC North. As for the magnitude of NECB, this might be related to the active fire regime in the region (fig. 6.6*A*). The variability of the projected change in NECB among the six climate simulations was the highest in the Western Alaska LCC (fig. 6.6*B*). The largest uncertainty in this region might not only be related to the uncertainty related to climate and disturbance forcings (uncertainty illustrated in chapter 2, section 2.4.6.1), but also to (1) the weakness of the parameterization and (or) (2) the lack of representation of processes that are at play specifically in this region. The lack of observations in the Western Alaska LCC compared with the other ecoregions greatly limits our current understanding of the drivers of carbon dynamics in the region (fig. 6.6*C*).

Table 6.9. Average vegetation and soil carbon stocks for the last decade (2090–2099) of the projection period and mean annual change in vegetation and soil carbon stocks between the last decades of the historical period (2000–2009) and the projection period (2090–2099) per Landscape Conservation Cooperative region for each of the six climate simulations.

[The six climate simulations are combinations of two general circulation models, version 3.1-T47 of the Coupled Global Climate Model (CGCM3.1) developed by the Canadian Centre for Climate Modelling and Analysis and version 5 of the European Centre Hamburg Model (ECHAM5) developed by the Max Planck Institute, and three climate scenarios of the Intergovernmental Panel on Climate Change's Special Report on Emissions Scenarios (Nakićenović and Swart, 2000), B1, A1B, and A2, in order of low to high projected CO_2 emissions. Data may not add to totals shown because of independent rounding. TgC, teragram of carbon]

Climate scenario	Landscape Conservation Cooperative (LCC) region	Vegetation carbon stocks (TgC)		Soil carbon stocks (TgC)	
		Average	Mean annual change	Average	Mean annual change
		CGCM3.1			
A1B	Arctic LCC	430	0.94	11,424	6.1
	Western Alaska LCC	1,219	1.61	20,591	8.2
	Northwest Boreal LCC North	1,496	2.50	6,942	2.7
	Northwest Boreal LCC South	494	–0.16	7,942	2.0
	North Pacific LCC	1,340	2.30	9,902	3.9
	Total	**4,979**	**7.19**	**56,801**	**23.0**
A2	Arctic LCC	432	0.98	11,227	4.0
	Western Alaska LCC	1,238	2.04	18,176	4.3
	Northwest Boreal LCC North	1,500	2.53	7,197	5.7
	Northwest Boreal LCC South	520	0.17	7,186	2.3
	North Pacific LCC	1,370	2.79	4,979	2.0
	Total	**5,060**	**8.52**	**48,765**	**18.4**
B1	Arctic LCC	410	0.82	10,929	6.9
	Western Alaska LCC	1,137	0.88	19,236	4.6
	Northwest Boreal LCC North	1,423	1.69	6,796	1.7
	Northwest Boreal LCC South	497	–0.09	7,229	1.8
	North Pacific LCC	1,284	1.81	5,115	3.6
	Total	**4,751**	**5.11**	**49,305**	**18.6**
		ECHAM5			
A1B	Arctic LCC	473	1.41	11,106	3.0
	Western Alaska LCC	1,313	2.63	19411	–2.5
	Northwest Boreal LCC North	1,585	3.50	7,023	3.8
	Northwest Boreal LCC South	518	0.11	7,857	1.4
	North Pacific LCC	1,391	2.85	9,628	0.8
	Total	**5,281**	**10.50**	**55,024**	**6.5**
A2	Arctic LCC	473	1.45	11,190	3.8
	Western Alaska LCC	1,293	2.60	18,201	–0.6
	Northwest Boreal LCC North	1,600	3.65	7,079	4.3
	Northwest Boreal LCC South	526	0.24	6,974	1.0
	North Pacific LCC	1,343	2.47	4,856	0.8
	Total	**5,235**	**10.41**	**48,301**	**9.2**
B1	Arctic LCC	426	0.88	11,165	3.5
	Western Alaska LCC	1,226	1.87	17,815	–1.7
	Northwest Boreal LCC North	1,564	3.25	6,942	2.6
	Northwest Boreal LCC South	506	0.00	7,131	0.8
	North Pacific LCC	1,301	2.00	4,931	1.6
	Total	**5,024**	**8.01**	**47,984**	**6.7**

Table 6.10. Average annual vegetation and soil carbon fluxes for the last decade of the projection period (2090–2099) and mean annual change in net ecosystem carbon balance between the last decades of the historical period (2000–2009) and the projection period (2090–2099) per Landscape Conservation Cooperative region for each of the six climate simulations.

[The six climate simulations are combinations of two general circulation models, version 3.1-T47 of the Coupled Global Climate Model (CGCM3.1) developed by the Canadian Centre for Climate Modelling and Analysis and version 5 of the European Centre Hamburg Model (ECHAM5) developed by the Max Planck Institute, and three climate scenarios of the Intergovernmental Panel on Climate Change's Special Report on Emissions Scenarios (Nakićenović and Swart, 2000), B1, A1B, and A2, in order of low to high projected CO_2 emissions. Data may not add to totals or compute to net ecosystem carbon balance shown because of independent rounding. TgC/yr, teragram of carbon per year; $TgCO_2$-eq/yr, teragram of carbon dioxide equivalent per year]

Climate scenario	Landscape Conservation Cooperative (LCC) region	Net primary productivity (TgC/yr)	Hetero-trophic respiration (TgC/yr)	Fire emissions ($CO+CO_2$) (TgC/yr)	Pyrogenic methane emissions ($TgCO_2$-eq/yr)	Methane uptake ($TgCO_2$-eq/yr)	Net ecosystem carbon balance (TgC/yr)	Global warming potential ($TgCO_2$-eq/yr)	Mean annual change in net ecosystem carbon balance (TgC/yr)
				CGCM3.1					
A1B	Arctic LCC	40.7	33.6	0.1	0.01	-7.32×10^{-4}	7.02	–25.8	0.044
	Western Alaska LCC	74.0	53.7	10.5	1.06	-2.19×10^{-3}	9.84	–35.1	0.061
	Northwest Boreal LCC North	78.0	64.1	8.8	0.81	-3.99×10^{-4}	5.17	–18.2	0.115
	Northwest Boreal LCC South	24.0	20.0	2.2	0.21	-5.32×10^{-4}	1.88	–6.7	0.013
	North Pacific LCC	32.9	26.6	0.0	0.00	-1.50×10^{-4}	6.24	–22.9	0.041
	Total	**249.7**	**198.0**	**21.5**	**2.09**	**-3.99×10^{-3}**	**30.15**	**–108.7**	**0.274**
A2	Arctic LCC	45.7	21.9	18.7	1.93	-9.31×10^{-4}	5.02	–16.7	0.020
	Western Alaska LCC	78.1	23.9	47.8	4.89	-3.23×10^{-3}	6.34	–18.9	0.028
	Northwest Boreal LCC North	76.8	55.9	12.7	1.21	-5.32×10^{-3}	8.21	–29.0	0.148
	Northwest Boreal LCC South	25.4	15.3	7.5	0.76	-1.30×10^{-3}	2.51	–8.5	0.022
	North Pacific LCC	36.3	25.4	6.0	0.64	-1.80×10^{-4}	4.80	–17.0	0.025
	Total	**262.3**	**142.4**	**92.7**	**9.44**	**-1.10×10^{-2}**	**26.87**	**–90.1**	**0.243**
B1	Arctic LCC	41.0	33.3	0.1	0.01	-5.65×10^{-4}	7.69	–28.2	0.057
	Western Alaska LCC	69.9	52.4	12.0	1.19	-2.23×10^{-3}	5.48	–19.0	0.020
	Northwest Boreal LCC North	73.5	62.0	8.2	0.76	-3.23×10^{-3}	3.39	–11.8	0.096
	Northwest Boreal LCC South	23.0	16.0	5.3	0.54	-7.98×10^{-4}	1.74	–5.9	0.013
	North Pacific LCC	29.8	24.3	0.0	0.00	-7.65×10^{-5}	5.46	–20.0	0.031
	Total	**237.2**	**187.9**	**25.5**	**2.49**	**-6.98×10^{-3}**	**23.75**	**–84.9**	**0.216**
				ECHAM5					
A1B	Arctic LCC	51.3	24.1	22.7	2.33	-1.13×10^{-3}	4.42	–14.1	0.013
	Western Alaska LCC	83.3	26.3	56.8	5.82	-3.16×10^{-3}	0.10	4.9	−0.050
	Northwest Boreal LCC North	79.6	59.8	12.5	1.18	-5.65×10^{-3}	7.29	–25.7	0.138
	Northwest Boreal LCC South	25.9	15.0	9.4	0.94	-1.33×10^{-3}	1.55	–4.8	0.010
	North Pacific LCC	38.1	24.6	9.8	1.04	-2.09×10^{-4}	3.68	–12.6	0.013
	Total	**278.3**	**149.7**	**111.2**	**11.34**	**-1.16×10^{-2}**	**17.04**	**–52.4**	**0.124**
A2	Arctic LCC	51.2	23.9	22	2.27	-1.13×10^{-3}	5.21	–17.1	0.023
	Western Alaska LCC	84.1	35.3	46.6	4.78	-5.32×10^{-3}	1.97	–3.0	−0.022
	Northwest Boreal LCC North	81.2	61.4	11.9	1.11	-6.32×10^{-3}	7.91	–28.0	0.144
	Northwest Boreal LCC South	26.2	14.5	10.4	1.05	-1.83×10^{-3}	1.25	–3.6	0.008
	North Pacific LCC	33.8	26.2	4.3	0.45	-2.69×10^{-4}	3.24	–11.5	0.006
	Total	**276.5**	**161.3**	**95.3**	**9.66**	**-1.50×10^{-2}**	**19.57**	**–63.1**	**0.159**
B1	Arctic LCC	42.4	30.5	7.6	0.78	-7.65×10^{-4}	4.33	–15.2	0.012
	Western Alaska LCC	70.0	53.5	16.2	1.66	-2.63×10^{-3}	0.21	0.7	−0.041
	Northwest Boreal LCC North	74.1	63.5	4.8	0.45	-3.66×10^{-3}	5.81	–20.9	0.121
	Northwest Boreal LCC South	22.9	18.5	3.6	0.36	-8.31×10^{-4}	0.77	–2.5	0.002
	North Pacific LCC	31.5	24.1	3.8	0.40	-7.98×10^{-5}	3.60	–12.9	0.011
	Total	**240.9**	**190.1**	**36.0**	**3.66**	**-7.98×10^{-3}**	**14.72**	**–50.7**	**0.105**

Table 6.11. Change in decadal averages of mean annual net ecosystem carbon balance between the last decades of the historical period (2000–2009) and projection period (2090–2099) compared with corresponding changes in mean annual temperature, total annual precipitation, mean annual atmospheric carbon dioxide, (CO_2) concentration, and total area burned for each of the six climate change simulations.

[The six climate simulations are combinations of two general circulation models, version 3.1-T47 of the Coupled Global Climate Model (CGCM3.1) developed by the Canadian Centre for Climate Modelling and Analysis and version 5 of the European Centre Hamburg Model (ECHAM5) developed by the Max Planck Institute, and three climate scenarios of the Intergovernmental Panel on Climate Change's Special Report on Emissions Scenarios (Nakićenović and Swart, 2000), B1, A1B, and A2, in order of low to high projected CO_2 emissions. $gC/m^2/yr$, gram of carbon per square meter per year; °C/yr, degree Celsius per year; mm/yr, millimeter per year; ppm/yr, part per million per year; km^2, square kilometer]

Climate scenario	Change in mean annual net ecosystem carbon balance ($gC/m^2/yr$)	Change in mean annual temperature (°C/yr)	Change in total annual precipitation (mm/yr)	Change in mean annual atmospheric CO_2 concentration (ppm/yr)	Change in total area burned (km^2)
CGCM3.1					
A1B	30.17	0.031	1.27	3.72	386,165
A2	25.23	0.046	2.19	4.92	448,945
B1	21.71	0.018	0.83	1.88	353,393
ECHAM5					
A1B	14.16	0.059	1.89	3.72	623,016
A2	17.01	0.061	1.62	4.92	607,247
B1	11.56	0.038	1.09	1.88	504,987

6.5. Conclusion: Carbon Dynamics in Upland Alaska

We have examined carbon dynamics in upland ecosystems of Alaska for the two time periods using a modeling framework coupling biogeographic-disturbance and biogeochemical models. Through the historical period 1950–2009, we used historical climate and disturbance records to simulate annual carbon dynamics through upland Alaska. The assessment was conducted at a 1-km spatial resolution, which is unprecedented for Alaska and allows for integrating the effect of medium-scale diversity in vegetation composition and physiography on regional carbon dynamics. We also projected the potential changes in carbon dynamics through 2099 using a set of climate simulations that best represent the range of warming scenarios for the region. This set of climate simulations allowed us to quantify the uncertainty of future carbon balance in upland Alaska associated with the variability of climate projections.

During the historical period, upland ecosystems in Alaska were gaining 5 TgC/yr of carbon to the ecosystem (NECB); all LCC regions were net carbon sinks, except for the Northwest Boreal LCC North where large carbon losses from wildfire (specifically during large fire years in 1956, 1969, 1977, and in the 1990s and 2000s) in addition to carbon loss from heterotrophic respiration offset carbon gain from net primary productivity. Pyrogenic CH_4 emissions during the historical period were not enough to offset the carbon gain at the State level. Global warming potentials were therefore negative in Alaskan upland ecosystems, with a net carbon sink of –16 $TgCO_2$-eq/yr on average. The historical carbon simulations were validated by comparing modeled vegetation and soil carbon stocks in arctic and boreal ecosystems with independent field observations. Proper validation was not possible for the maritime forests because of the lack of independent, site-specific observations available in the region. Although climate and disturbance history are quite well constrained by field observations at the regional level, uncertainty remains on land-cover distribution and dynamics

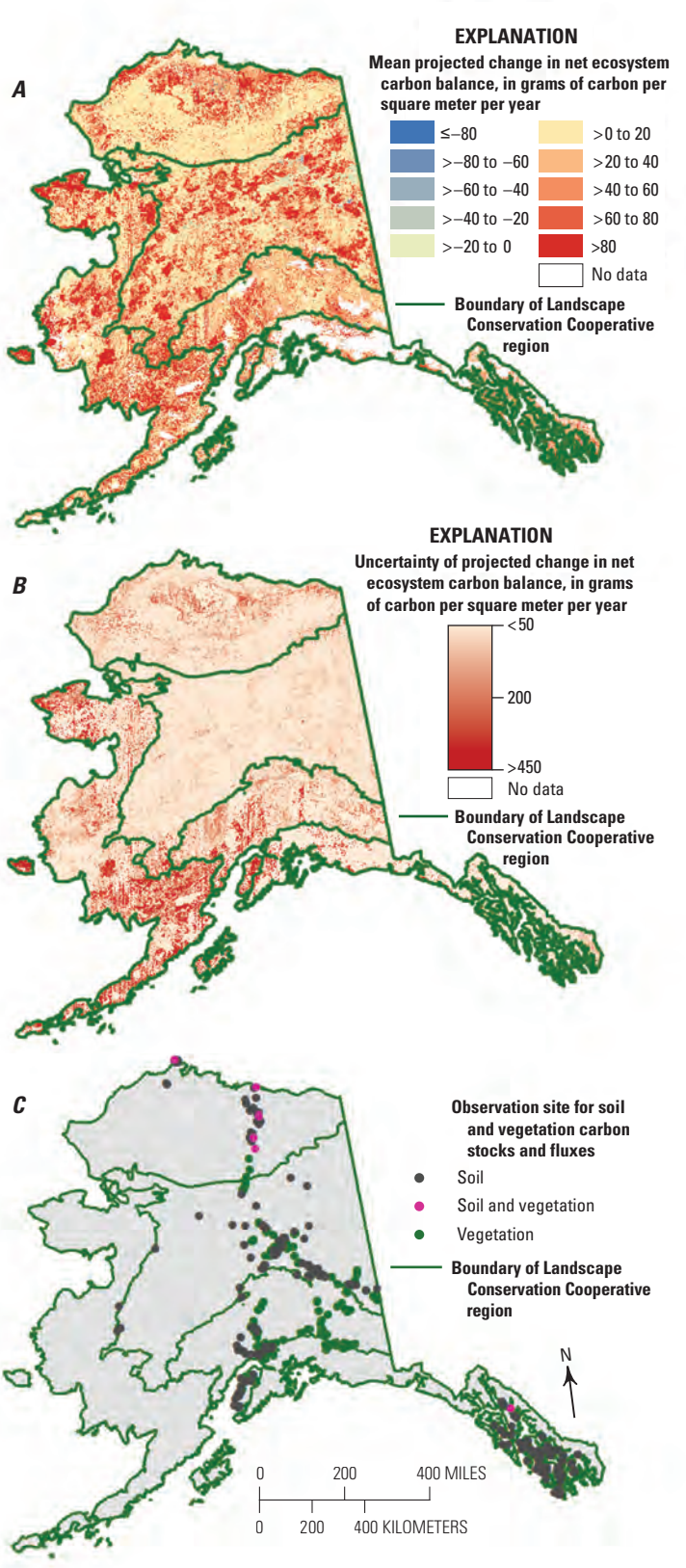

Figure 6.6. Spatial distribution of *A*, average mean change in net ecosystem carbon balance for all climate simulations between the last decades of the historical period (2000–2009) and the projection period (2090–2099) and *B*, corresponding uncertainty. *C*, Distribution of existing observation sites for soil and vegetation carbon stocks and fluxes.

in response to warming in the region. In the present assessment, vegetation was considered static through time. Future assessments may explore how the current vegetation distribution and the effect of fire and permafrost thaw on land cover will affect regional land carbon dynamics. Similarly, soil texture has a large effect on soil hydrologic fluxes that affect soil carbon and permafrost dynamics (see chapter 3), and large uncertainty remains on the spatial distribution of soil texture in Alaska (Liu and others, 2013).

During the projection period (2010–2099), all LCC regions of Alaska were projected to be carbon sinks. On average, upland ecosystems would store 22.0 TgC/yr, associated with the negative global warming potential of –75.0 $TgCO_2$-eq/yr (carbon sink) despite the projected increase in pyrogenic CH_4 emissions. The uncertainty of projected NECB associated with climate forcing would range from 14.7 to 30.2 TgC/yr statewide. Compared with the historical period, carbon storage in upland ecosystems was projected to increase between 0.105 and 0.274 TgC/yr by the end of the century. As shown in chapter 2, projected disturbance regimes associated with future climate changes are highly variable. The current assessment is based on a single disturbance scenario for each climate simulation that reproduces the best historical fire records. However, future assessments may explore the additional uncertainty of future carbon dynamics associated with multiple disturbance regimes.

6.6. References Cited

Alaback, P.B., 1982, Dynamics of understory biomass in Sitka spruce-western hemlock forests of southeast Alaska: Ecology, v. 63, no. 6, p. 1932–1948, http://dx.doi.org/10.2307/1940131.

Balshi, M.S., McGuire, A.D., Duffy, P., Flannigan, M., Kicklighter, D.W., and Melillo, J., 2009, Vulnerability of carbon storage in North American boreal forests to wildfires during the 21st century: Global Change Biology, v. 15, no. 6, p. 1491–1510, http://dx.doi.org/10.1111/j.1365-2486.2009.01877.x.

Balshi, M.S., McGuire, A.D., Zhuang, Q., Melillo, J., Kicklighter, D.W., Kasischke, E., Wirth, C., Flannigan, M., Harden, J., Clein, J.S., Burnside, T.J., McAllister, J., Kurz, W.A., Apps, M., and Shvidenko, A., 2007, The role of historical fire disturbance in the carbon dynamics of the pan-boreal region; A process-based analysis: Journal of Geophysical Research, v. 112, no. G2, article G02029, 18 p., http://dx.doi.org/10.1029/2006JG000380.

Binkley, Dan, 1982, Nitrogen fixation and net primary production in a young Sitka alder stand: Canadian Journal of Botany, v. 60, no. 3, p. 281–284, http://dx.doi.org/10.1139/b82-036.

Burn, C.R., Mackay, J.R., and Kokelj, S.V., 2009, The thermal regime of permafrost and its susceptibility to degradation in upland terrain near Inuvik, N.W.T.: Permafrost and Periglacial Processes, v. 20, no. 2, p. 221–227, http://dx.doi.org/10.1002/ppp.649.

Chapin, F.S., III, Woodwell, G.M., Randerson, J.T., Rastetter, E.B., Lovett, G.M., Baldocchi, D.D., Clark, D.A., Harmon, M.E., Schimel, D.S., Valentini, R., Wirth, C., Aber, J.D., Cole, J.J., Goulden, M.L., Harden, J.W., Heimann, M., Howarth, R.W., Matson, P.A., McGuire, A.D., Melillo, J.M., Mooney, H.A., Neff, J.C., Houghton, R.A., Pace, M.L., Ryan, M.G., Running, S.W., Sala, O.E., Schlesinger, W.H., and Schulze, E.-D., 2006, Reconciling carbon-cycle concepts, terminology, and methods: Ecosystems, v. 9, no. 7, p. 1041–1050, http://dx.doi.org/10.1007/s10021-005-0105-7.

Clein, J.S., McGuire, A.D., Zhang, X., Kicklighter, D.W., Melillo, J.M., Wofsy, S.C., Jarvis, P.G., and Massheder, J.M., 2002, Historical and projected carbon balance of mature black spruce ecosystems across North America; The role of carbon-nitrogen interactions: Plant and Soil, v. 242, no. 1, p. 15–32, http://dx.doi.org/10.1023/a:1019673420225.

Cole, E.C., Hanley, T.A., and Newton, Michael, 2010, Influence of precommercial thinning on understory vegetation of young-growth Sitka spruce forests in southeastern Alaska: Canadian Journal of Forest Research, v. 40, no. 4, p. 619–628, http://dx.doi.org/10.1139/X10-009.

Colt, Steve, Dugan, Darcy, and Fay, Ginny, 2007, The regional economy of southeast Alaska, final report, prepared for Alaska Conservation Foundation: Anchorage, Alaska, University of Alaska-Anchorage, Institute of Social and Economic Research, 134 p. [Also available at http://www.iser.uaa.alaska.edu/Publications/Southeast-EconomyOverviewfinal4.pdf.]

D'Amore, D.V., Fellman, J.B., Edwards, R.T., Hood, Eran, and Ping, C.-L., 2012, Hydropedology of the North American coastal temperate rainforest, *in* Lin, Henry, ed., Hydropedology; Synergystic integration of soil science and hydrology: Waltham, Mass., Academic Press, p. 351–380.

Deal, R.L., and Tappeiner, J.C., 2002, The effects of partial cutting on stand structure and growth of western hemlock–Sitka spruce stands in southeast Alaska: Forest Ecology and Management, v. 159, no. 3, p. 173–186, http://dx.doi.org/10.1016/S0378-1127(00)00727-1.

Dyrness, C.T., and Norum, R.A., 1983, The effects of experimental fires on black spruce forest floors in interior Alaska: Canadian Journal of Forest Research, v. 13, no. 5, p. 879–893, http://dx.doi.org/10.1139/x83-118.

Euskirchen, E.S., Bret-Harte, M.S., Scott, G.J., Edgar, C., Shaver, G.R., 2012, Seasonal patterns of carbon dioxide and water fluxes in three representative tundra ecosystems in northern Alaska: Ecosphere, v. 3, no. 1, article 4, 19 p., http://dx.doi.org/10.1890/ES11-00202.1.

Euskirchen, E.S., McGuire, A.D., and Chapin, F.S., III, 2007, Energy feedbacks of northern high-latitude ecosystems to the climate system due to reduced snow cover during 20th century warming: Global Change Biology, v. 13, no. 11, p. 2425–2438, http://dx.doi.org/10.1111/j.1365-2486.2007.01450.x.

Euskirchen, E.S., McGuire, A.D., Kicklighter, D.W., Zhuang, Q., Clein, J.S., Dargaville, R.J., Dye, D.G., Kimball, J.S., McDonald, K.C., Melillo, J.M., Romanovsky, V.E., and Smith, N.V., 2006, Importance of recent shifts in soil thermal dynamics on growing season length, productivity, and carbon sequestration in terrestrial high-latitude ecosystems: Global Change Biology, v. 12, no. 4, p. 731–750, http://dx.doi.org/10.1111/j.1365-2486.2006.01113.x.

Fisher, J.B., Sikka, M., Oechel, W.C., Huntzinger, D.N., Melton, J.R., Koven, C.D., Ahlström, A., Arain, M.A., Baker, I., Chen, J.M., Ciais, P., Davidson, C., Dietze, M., El-Masri, B., Hayes, D., Huntingford, C., Jain, A.K., Levy, P.E., Lomas, M.R., Poulter, B., Price, D., Sahoo, A.K., Schaefer, K., Tian, H., Tomelleri, E., Verbeeck, H., Viovy, N., Wania, R., Zeng, N., and Miller, C.E., 2014, Carbon cycle uncertainty in the Alaskan Arctic: Biogeosciences, v. 11, p. 4271–4288, http://dx.doi.org/10.5194/bg-11-4271-2014.

Flato, G.M., 2005, The third generation coupled global climate model (CGCM3) (and included links to the description of the AGCM3 atmospheric model): Canadian Centre for Climate Modelling and Analysis, available at http://ec.gc.ca/ccmac-cccma/default.asp?lang=En&n=1299529F-1.

French, N.H.F., Kasischke, E.S., and Williams, D.G., 2002, Variability in the emission of carbon-based trace gases from wildfire in the Alaskan boreal forest: Journal of Geophysical Research; Atmospheres, v. 107, no. D1, p. FFR 7–1 to FFR 7–11, http://dx.doi.org/10.1029/2001JD000480.

Genet, H., McGuire, A.D., Barrett, K., Breen, A., Euskirchen, E.S., Johnstone, J.F., Kasischke, E.S., Melvin, A.M., Bennett, A., Mack, M.C., Rupp, T.S., Schuur, E.A.G., Turetsky, M.R., and Yuan, F., 2013, Modeling the effects of fire severity and climate warming on active layer thickness and soil carbon storage of black spruce forests across the landscape in interior Alaska: Environmental Research Letters, v. 8, no. 4, letter 045016, 13 p., http://dx.doi.org/10.1088/1748-9326/8/4/045016.

Gillett, N.P., Weaver, A.J., Zwiers, F.W., and Flannigan, M.D., 2004, Detecting the effect of climate change on Canadian forest fires: Geophysical Research Letters, v. 31, no. 18, letter L18211, 4 p., http://dx.doi.org/10.1029/2004GL020876.

Global Soil Data Task Group, 2000, Global Gridded Surfaces of Selected Soil Characteristics (IGBP–DIS [International Geosphere-Biosphere Programme–Data and Information System]) dataset: Oak Ridge, Tenn., Oak Ridge National Laboratory Distributed Active Archive Center, http://dx.doi.org/10.3334/ORNLDAAC/569.

Gough, Laura, and Hobbie, S.E., 2003, Responses of moist non-acidic arctic tundra to altered environment; Productivity, biomass, and species richness: Oikos, v. 103, no. 1, p. 204–216, http://dx.doi.org/10.1034/j.1600-0706.2003.12363.x.

Gough, Laura, Moore, J.C., Shaver, G.R., Simpson, R.T., and Johnson, D.R., 2012, Above- and belowground responses of arctic tundra ecosystems to altered soil nutrients and mammalian herbivory: Ecology, v. 93, no. 7, p. 1683–1694, http://dx.doi.org/10.1890/11-1631.1.

Grosse, Guido, Harden, Jennifer, Turetsky, Merritt, McGuire, A.D., Camill, Philip, Tarnocai, Charles, Frolking, Steve, Schuur, E.A.G., Jorgenson, Torre, Marchenko, Sergei, Romanovsky, Vladimir, Wickland, K.P., French, Nancy, Waldrop, Mark, Bourgeau-Chavez, Laura, and Streigl, R.G., 2011, Vulnerability of high latitude soil carbon in North America to disturbance: Journal of Geophysical Research; Biogeosciences, v. 116, no. G4, article G00K06, 23 p., http://dx.doi.org/10.1029/2010JG001507.

Gustine, D.D., Brinkman, T.J., Lindgren, M.A., Schmidt, J.I., Rupp, T.S., and Adams, L.G., 2014, Climate-driven effects of fire on winter habitat for caribou in the Alaskan-Yukon Arctic: PLOS ONE, v. 9, no. 7, article e100588, 11 p., http://dx.doi.org/10.1371/journal.pone.0100588.

Harris, I., Jones, P.D., Osborn, T.J., and Lister, D.H., 2014, Updated high-resolution grids of monthly climatic observations—the CRU TS3.10 dataset: International Journal of Climatology, v. 34, no. 3, p. 623–642, http://dx.doi.org/10.1002/joc.3711.

Hay, L.E., Wilby, R.L., and Leavesley, G.H., 2000, A comparison of delta change and downscaled GCM scenarios for three mountainous basins in the United States: Journal of the American Water Resources Association, v. 36, no. 2, p. 387–397, http://dx.doi.org/10.1111/j.1752-1688.2000.tb04276.x.

Hayes, D.J., McGuire, A.D., Kicklighter, D.W., Gurney, K.R., Burnside, T.J., and Melillo, J.M., 2011, Is the northern high-latitude land-based CO_2 sink weakening?: Global Biogeochemical Cycles, v. 25, no. 3, article GB3018, 14 p., http://dx.doi.org/10.1029/2010gb003813.

Hayhoe, K.A., 2010, A standardized framework for evaluating the skill of regional climate downscaling techniques: Urbana-Champaign, Ill., University of Illinois, Ph.D. dissertation, 153 p. [Also available at http://hdl.handle.net/2142/16044.]

Johnson, K.D., Harden, Jennifer, McGuire, A.D., Bliss, N.B., Bockheim, J.G., Clark, Mark, Nettleton-Hollingsworth, Teresa, Jorgenson, M.T., Kane, E.S., Mack, Michelle, O'Donnell, Jonathan, Ping, C.-L., Schuur, E.A.G., Turetsky, M.R., and Valentine, D.W., 2011, Soil carbon distribution in Alaska in relation to soil-forming factors Geoderma, v. 167–168, p. 71–84, http://dx.doi.org/10.1016/j.geoderma.2011.10.006.

Johnstone, J.F., Rupp, T.S., Olson, Mark, and Verbyla, David, 2011, Modeling impacts of fire severity on successional trajectories and future fire behavior in Alaskan boreal forests: Landscape Ecology, v. 26, no. 4, p. 487–500, http://dx.doi.org/10.1007/s10980-011-9574-6.

Kasischke, E.S., and Turetsky, M.R., 2006, Recent changes in the fire regime across the North American boreal region—Spatial and temporal patterns of burning across Canada and Alaska: Geophysical Research Letters, v. 33, no. 9, letter L09703, 5 p., http://dx.doi.org/10.1029/2006GL025677.

Kasischke, E.S., Verbyla, D.L., Rupp, T.S., McGuire, A.D., Murphy, K.A., Jandt, Randi, Barnes, J.L., Hoy, E.E., Duffy, P.A., Calef, Monika, and Turetsky, M.R., 2010, Alaska's changing fire regime—Implications for the vulnerability of its boreal forests: Canadian Journal of Forest Research, v. 40, no. 7, p. 1313–1324, http://dx.doi.org/10.1139/X10-098.

Kasischke, E.S., Williams, David, and Barry, Donald, 2002, Analysis of the patterns of large fires in the boreal forest region of Alaska: International Journal of Wildland Fire, v. 11, no. 2, p. 131–144, http://dx.doi.org/10.1071/WF02023.

Liu, S., Wei, Y., Post, W.M., Cook, R.B., Schaefer, K., and Thornton, M.M., 2013, The Unified North American Soil Map and its implication on the soil organic carbon stock in North America: Biogeosciences, v. 10, no. 5, p. 2915–2930, http://dx.doi.org/10.5194/bg-10-2915-2013.

Mack, M.C., Bret-Harte, M.S., Hollingsworth, T.N., Jandt, R.R., Schuur, E.A.G., Shaver, G.R., and Verbyla, D.L., 2011, Carbon loss from an unprecedented Arctic tundra wildfire: Nature, v. 475, no. 7357, p. 489–492, http://dx.doi.org/10.1038/nature10283.

Malone, Thomas, Liang, Jingjing, and Packee, E.C., 2009, Cooperative Alaska Forest Inventory: U.S. Department of Agriculture, Forest Service, Pacific Northwest Research Station, General Technical Report PNW–GTR–785, 42 p. [Also available at http://www.fs.fed.us/pnw/pubs/pnw_gtr785.pdf.]

Mann, D.H., Rupp, T.S., Olson, M.A., and Duffy, P.A., 2012, Is Alaska's boreal forest now crossing a major ecological threshold?: Arctic, Antarctic, and Alpine Research, v. 44, no. 3, p. 319–331, http://dx.doi.org/10.1657/1938-4246-44.3.319.

McFarlane, N.A., Boer, G.J., Blanchet, J.-P., and Lazare, M., 1992, The Canadian Climate Centre second-generation general circulation model and its equilibrium climate: Journal of Climate, v. 5, no. 10, p. 1013–1044, http://dx.doi.org/10.1175/1520-0442(1992)005<1013:TCCCSG>2.0.CO;2.

McGuire, A.D., Anderson, L.G., Christensen, T.R., Dallimore, Scott, Guo, Laodong, Hayes, D.J., Heimann, Martin, Lorenson, T.D., Macdonald, R.W., and Roulet, Nigel, 2009, Sensitivity of the carbon cycle in the Arctic to climate change: Ecological Monographs, v. 79, no. 4, p. 523–555, http://dx.doi.org/10.1890/08-2025.1.

McGuire, A.D., Christensen, T.R., Hayes, D., Heroult, A., Euskirchen, E., Kimball, J.S., Koven, C., Lafleur, P., Miller, P.A., Oechel, W., Peylin, P., Williams, M., and Yi, Y., 2012, An assessment of the carbon balance of Arctic tundra; Comparisons among observations, process models, and atmospheric inversions: Biogeosciences, v. 9, p. 3185–3204, http://dx.doi.org/10.5194/bg-9-3185-2012.

McGuire, A.D., Hayes, D.J., Kicklighter, D.W., Manizza, M., Zhuang, Q., Chen, M., Follows, M.J., Gurney, K.R., McClelland, J.W., Melillo, J.M., Peterson, B.J., and Prinn, R.G., 2010, An analysis of the carbon balance of the Arctic Basin from 1997 to 2006: Tellus; Series B, Chemical and Physical Meteorology, v. 62B, no. 5, p. 455–474, http://dx.doi.org/10.1111/j.1600-0889.2010.00497.x.

McGuire, A.D., Melillo, J.M., Joyce, L.A., Kicklighter, D.W., Grace, A.L., Moore, B., III, and Vorosmarty, C.J., 1992, Interactions between carbon and nitrogen dynamics in estimating net primary productivity for potential vegetation in North America: Global Biogeochemical Cycles, v. 6, no. 2, p. 101–124, http://dx.doi.org/10.1029/92GB00219.

Nakićenović, Nebojša, and Swart, Robert, eds., 2000, Special report on emissions scenarios—A special report of Working Group III of the Intergovernmental Panel on Climate Change: Cambridge, United Kingdom, Cambridge University Press, 599 p., accessed [date], at http://www.ipcc.ch/ipccreports/sres/emission/index.php?idp=0.

Pan, Yude, Birdsey, R.A., Fang, Jingyun, Houghton, Richard, Kauppi, P.E., Kurz, W.A., Phillips, O.L., Shvidenko, Anatoly, Lewis, S.L., Canadell, J.G., Ciais, Philippe, Jackson, R.B., Pacala, S.W., McGuire, A.D., Piao, Shilong, Rautiainen, Aapo, Sitch, Stephen, and Hayes, Daniel, 2011, A large and persistent carbon sink in the world's forests: Science, v. 333, no. 6045, p. 988–993, http://dx.doi.org/10.1126/science.1201609.

Raich, J.W., Rastetter, E.B., Melillo, J.M., Kicklighter, D.W., Steudler, P.A., Peterson, B.J., Grace, A.L., Moore, B., III, and Vörösmarty, C.J., 1991, Potential net primary productivity in South America; Application of a global model: Ecological Applications, v. 1, no. 4, p. 399–429, http://dx.doi.org/10.2307/1941899.

Rakestraw, L.W., 1981, A history of the United States Forest Service in Alaska: Anchorage, Alaska, U.S. Department of Agriculture Forest Service, 137 p.

Rastetter, E.B., King, A.W., Cosby, B.J., Hornberger, G.M., O'Neill, R.V., and Hobbie, J.E., 1992, Aggregating fine-scale ecological knowledge to model coarser-scale attributes of ecosystems: Ecological Applications, v. 2, no. 1, p. 55–70, http://dx.doi.org/10.2307/1941889.

Roeckner, E., Bäuml, G., Bonaventura, L., Brokopf, R., Esch, M., Giorgetta, M., Hagemann, S., Kirchner, I., Kornblueh, L., Manzini, E., Rhodin, A., Schlese, U., Schulzweida, U., and Tompkins, A., 2003, The atmospheric general circulation model ECHAM5, part I—Model description: Max-Planck-Institut für Meteorologie Report, no. 349, 127 p. [Also available at https://www.mpimet.mpg.de/fileadmin/publikationen/Reports/max_scirep_349.pdf.]

Roeckner, E., Brokopf, R., Esch, M., Giorgetta, M., Hagemann, S., Kornblueh, L., Manzini, E., Schlese, U., and Schulzweida, U., 2004, The atmospheric general circulation model ECHAM5, part II—Sensitivity of simulated climate to horizontal and vertical resolution: Max-Planck-Institut für Meteorologie Report No. 354, 56 p. [Also available at http://pubman.mpdl.mpg.de/pubman/item/escidoc:995221:8/component/escidoc:995220/MPI_Report354.pdf.]

Ruess, R.W., Van Cleve, K., Yarie, J., Viereck, L.A., 1996, Contributions of fine root production and turnover to the carbon and nitrogen cycling in taiga forests of the Alaskan interior: Canadian Journal of Forest Research, v. 26, no. 8, p. 1326–1336, http://dx.doi.org/10.1139/x26-148.

Rupp, T.S., Chen, Xi, Olson, Mark, and McGuire, A.D., 2007, Sensitivity of simulated boreal fire dynamics to uncertainties in climate drivers: Earth Interactions, v. 11, no. 3, p. 1–21, http://dx.doi.org/10.1175/EI189.1.

Rupp, T.S., Starfield, A.M., and Chapin, F.S., III, 2000, A frame-based spatially explicit model of subarctic vegetation response to climatic change; Comparison with a point model: Landscape Ecology, v. 15, no. 4, p. 383–400, http://dx.doi.org/10.1023/A:1008168418778.

Rupp, T.S., Starfield, A.M., Chapin, F.S., III, and Duffy, P., 2002, Modeling the impact of black spruce on the fire regime of Alaskan boreal forest: Climatic Change, v. 55, no. 1–2, p. 213–233, http://dx.doi.org/10.1023/A:1020247405652.

Schaefer, Kevin, Zhang, Tingjin, Bruhwiler, Lori, and Barrett, A.P., 2011, Amount and timing of permafrost carbon release in response to climate warming: Tellus; Series B, Chemical and Physical Meteorology, v. 63B, no. 2, p. 165–180, http://dx.doi.org/10.1111/j.1600-0889.2011.00527.x.

Schuur, E.A.G., Abbott, B.W., Bowden, W.B., Brovkin, V., Camill, P., Canadell, J.G., Chanton, J.P., Chapin, F.S., III, Christensen, T.R., Ciais, P., Crosby, B.T., Czimczik, C.I., Grosse, G., Harden, J., Hayes, D.J., Hugelius, G., Jastrow, J.D., Jones, J.B., Kleinen, T., Koven, C.D., Krinner, G., Kuhry, P., Lawrence, D.M., McGuire, A.D., Natali, S.M., O'Donnell, J.A., Ping, C.L., Riley, W.J., Rinke, A., Romanovsky, V.E., Sannel, A.B.K., Schädel, C., Schaefer, K., Sky, J., Subin, Z.M., Tarnocai, C., Turetsky, M.R., Waldrop, M.P., Walter Anthony, K.M., Wickland, K.P., Wilson, C.J., and Zimov, S.A., 2013, Expert assessment of vulnerability of permafrost carbon to climate change: Climatic Change, v. 119, no. 2, p. 359–374, http://dx.doi.org/10.1007/s10584-013-0730-7.

Schuur, E.A.G., Bockheim, James, Canadell, J.G., Euskirchen, Eugenie, Field, C.B., Goryachkin, S.V., Hagemann, Stefan, Kuhry, Peter, Lafleur, P.M., Lee, Hanna, Mazhitova, Galina, Nelson, F.E., Rinke, Annette, Romanovsky, V.E., Shiklomanov, Nikolay, Tarnocai, Charles, Venevsky, Sergey, Vogel, J.G., and Zimov, S.A., 2008, Vulnerability of permafrost carbon to climate change; Implications for the global carbon cycle: BioScience, v. 58, no. 8, p. 701–714, http://dx.doi.org/10.1641/B580807.

Schuur, E.A.G., Vogel, J.G., Crummer, K.G., Lee, Hanna, Sickman, J.O., and Osterkamp, T.E., 2009, The effect of permafrost thaw on old carbon release and net carbon exchange from tundra: Nature, v. 459, no. 7246, p. 556–559, http://dx.doi.org/10.1038/nature08031.

Shaver, G.R., and Chapin, F.S., III, 1986, Effect of fertilizer on production and biomass of tussock tundra, Alaska, U.S.A.: Arctic and Alpine Research, v. 18, no. 3, p. 261–268. [Also available at http://dx.doi.org/10.2307/1550883.]

Shaver, G.R., and Chapin, F.S., III, 1991, Production; Biomass relationships and element cycling in contrasting arctic vegetation types: Ecological Monographs, v. 61, no. 1, p. 1–31, http://dx.doi.org/10.2307/1942997.

Sistla, S.A., Moore, J.C., Simpson, R.T., Gough, Laura, Shaver, G.R., and Schimel, J.P., 2013, Long-term warming restructures Arctic tundra without changing net soil carbon storage: Nature, v. 497, no. 7451, p. 615–618, http://dx.doi.org/10.1038/nature12129.

Sullivan, P.F., Sommerkorn, Martin, Rueth, H.M., Nadelhoffer, K.J., Shaver, G.R., and Welker, J.M., 2007, Climate and species affect fine root production with long-term fertilization in acidic tussock tundra near Toolik Lake, Alaska: Oecologia, v. 153, no. 3, p. 643–652, http://dx.doi.org/10.1007/s00442-007-0753-8.

Tarnocai, C., Canadell, J.G., Schuur, E.A.G., Kuhry, P., Mazhitova, G., and Zimov, S., 2009, Soil organic carbon pools in the northern circumpolar permafrost region: Global Biogeochemical Cycles, v. 23, no. 2, article GB2023, 11 p., http://dx.doi.org/10.1029/2008GB003327.

Turetsky, M.R., Kane, E.S., Harden, J.W., Ottmar, R.D., Manies, K.L., Hoy, Elizabeth, and Kasischke, E.S., 2011, Recent acceleration of biomass burning and carbon losses in Alaskan forests and peatlands: Nature Geoscience, v. 4, no. 1, p. 27–31, http://dx.doi.org/10.1038/ngeo1027.

van den Pol-van Dasselaar, A., van Beusichem, M.L., and Oenema, O., 1998, Effects of soil moisture content and temperature on methane uptake by grasslands on sandy soils: Plant and Soil, v. 204, no. 2, p. 213–22, http://dx.doi.org/10.1023/A:1004371309361.

Van Wijk, M.T., Williams, M., Gough, L., Hobbie, S.E., and Shaver, G.R., 2003, Luxury consumption of soil nutrients; A possible competitive strategy in above-ground and below-ground biomass allocation and root morphology for slow-growing arctic vegetation?: Journal of Ecology, v. 91, no. 4, p. 664–676, http://dx.doi.org/10.1046/j.1365-2745.2003.00788.x.

Weinstock, Bernard, 1969, Carbon monoxide—Residence time in the atmosphere: Science, v. 166, no. 3902, p. 224–225, http://dx.doi.org/10.1126/science.166.3902.224.

Whalen, S.C., and Reeburgh, W.S., 1990, Consumption of atmospheric methane by tundra soils: Nature, v. 346, no. 6280, p. 160–162, http://dx.doi.org/10.1038/346160a0.

Wickland, K.P., Neff, J.C., and Harden, J.W., 2010, The role of soil drainage class in carbon dioxide exchange and decomposition in boreal black spruce (*Picea mariana*) forest stands: Canadian Journal of Forest Research, v. 40, no. 11, p. 2123–2134, http://dx.doi.org/10.1139/X10-163.

Woo, M.-K., Arain, M.A., Mollinga, M., and, Yi, S., 2004, A two-directional freeze and thaw algorithm for hydrologic and land surface modelling: Geophysical Research Letters, v. 31, no. 12, letter L12501, 4 p., http://dx.doi.org/10.1029/2004GL019475.

Yi, Shuhua, Arain, M.A., and Woo, M.-K., 2006, Modifications of a land surface scheme for improved simulation of ground freeze-thaw in northern environments: Geophysical Research Letters, v. 33, no. 13, letter L13501, 5 p., http://dx.doi.org/10.1029/2006GL026340.

Yi, Shuhua, Manies, Kristen, Harden, Jennifer, and McGuire, A.D., 2009, Characteristics of organic soil in black spruce forests; Implications for the application of land surface and ecosystem models in cold regions: Geophysical Research Letters, v. 36, no. 5, letter L05501, 5 p., http://dx.doi.org/10.1029/2008GL037014.

Yi, Shuhua, McGuire, A.D., Harden, Jennifer, Kasischke, Eric, Manies, Kristen, Hinzman, Larry, Liljedahl, Anna, Randerson, Jim, Liu, Heping, Romanovsky, Vladimir, Marchenko, Sergei, and Kim, Yongwon, 2009, Interactions between soil thermal and hydrological dynamics in the response of Alaska ecosystems to fire disturbance: Journal of Geophysical Research; Biogeosciences, v. 114, no. G2, article G02015, 20 p., http://dx.doi.org/10.1029/2008JG000841.

Yi, Shuhua, McGuire, A.D., Kasischke, Eric, Harden, Jennifer, Manies, Kristen, Mack, Michelle, and Turetsky, Merritt, 2010, A dynamic organic soil biogeochemical model for simulating the effects of wildfire on soil environmental conditions and carbon dynamics of black spruce forests: Journal of Geophysical Research; Biogeosciences, v. 115, no. G4, article G04015, 15 p., http://dx.doi.org/10.1029/2010JG001302.

Yonemura, S., Kawashima, S., Tsuruta, H., 2000, Carbon monoxide, hydrogen, and methane uptake by soils in a temperate arable field and a forest: Journal of Geophysical Research; Atmospheres, v. 105, no. D11, p. 14347–14362.

Yoshikawa, Kenji, Bolton, W.R., Romanovsky, V.E., Fukuda, Masami, and Hinzman, L.D., 2002, Impacts of wildfire on the permafrost in the boreal forests of interior Alaska: Journal of Geophysical Research; Atmospheres, v. 107, no. D1, p. FFR 4–1 to FFR 4–14, http://dx.doi.org/10.1029/2001JD000438.

Yuan, F.-M., Yi, S.-H., McGuire, A.D., Johnson, K.D., Liang, J., Harden, J.W., Kasischke, E.S., and Kurz, W.A., 2012, Assessment of boreal forest historical C dynamics in the Yukon River Basin; Relative roles of warming and fire regime change: Ecological Applications, v. 22, no. 8, p. 2091–2109, http://dx.doi.org/10.1890/11-1957.1.

Zhuang, Q., McGuire, A.D., Melillo, J.M., Clein, J.S., Dargaville, R.J., Kicklighter, D.W., Myneni, R.B., Dong, J., Romanovsky, V.E., Harden, J., and Hobbie, J.E., 2003, Carbon cycling in extratropical terrestrial ecosystems of the Northern Hemisphere during the 20th century; A modeling analysis of the influences of soil thermal dynamics: Tellus; Series B, Chemical and Physical Meteorology, v. 55B, no. 3, p. 751–776, http://dx.doi.org/10.1034/j.1600-0889.2003.00060.x.

Zhuang, Q., McGuire, A.D., O'Neill, K.P., Harden, J.W., Romanovsky, V.E., and Yarie, J., 2002, Modeling soil thermal and carbon dynamics of a fire chronosequence in interior Alaska: Journal of Geophysical Research; Atmospheres, v. 107, no. D1, p. FFR 3–1 to FFR 3–26, http://dx.doi.org/10.1029/2001JD001244.

Zhuang, Q., Melillo, J.M., Kicklighter, D.W., Prinn, R.G., McGuire, A.D., Steudler, P.A., Felzer, B.S., and Hu, S., 2004, Methane fluxes between terrestrial ecosystems and the atmosphere at northern high latitudes during the past century; A retrospective analysis with a process-based biogeochemistry model: Global Biogeochemical Cycles, v. 18, no. 3, article GB3010, 23 p., http://dx.doi.org/10.1029/2004gb002239.

Zhuang, Q., Romanovsky, V.E., and McGuire, A.D., 2001, Incorporation of a permafrost model into a large-scale ecosystem model; Evaluation of temporal and spatial scaling issues in simulating soil thermal dynamics: Journal of Geophysical Research; Atmospheres, v. 106, no. D24, p. 33649–33670, http://dx.doi.org/10.1029/2001jd900151.

Zimov, S.A., Schuur, E.A.G., and Chapin, F.S., III, 2006, Permafrost and the global carbon budget: Science, v. 312, no. 5780, p. 1612–1613, http://dx.doi.org/10.1126/science.1128908.